Enhanced Secondary- and Hormone Metabolism in Leaves of Arbuscular Mycorrhizal *Medicago truncatula*[1[OPEN]]

Lisa Adolfsson,[a,2] Hugues Nziengui,[a,2] Ilka N Abreu,[b,3] Jan Šimura,[c,3] Azeez Beebo,[a,3] Andrei Herdean,[a] Jila Aboalizadeh,[a] Jitka Široká,[c] Thomas Moritz,[b] Ondřej Novák,[c] Karin Ljung,[b] Benoît Schoefs,[d] and Cornelia Spetea[a,4]

[a]Department of Biological and Environmental Sciences, University of Gothenburg, 405 30 Gothenburg, Sweden
[b]Umeå Plant Science Centre, Department of Forest Genetics and Plant Physiology, Swedish University of Agricultural Sciences, 901 83 Umea, Sweden
[c]Laboratory of Growth Regulators, Centre of the Region Haná for Biotechnological and Agricultural Research, Institute of Experimental Botany of Czech Academy of Sciences and Faculty of Science of Palacký University, CZ-78371 Olomouc, Czech Republic
[d]Metabolism, Engineering of Microalgal Molecules and Applications, Mer Molécules Santé, University Bretagne Loire, Institut Universitaire Mer et Littoral - Fédération de Recherche 3473 Centre National de la Recherche Scientifique, University of Le Mans, 72085 Le Mans cedex 9, France

ORCID IDs: 0000-0003-2314-8748 (H.N.); 0000-0003-4728-0161 (I.N.A.); 0000-0003-2143-0213 (A.H.); 0000-0002-4258-3190 (T.M.); 0000-0003-3452-0154 (O.N.); 0000-0003-2901-189X (K.L.); 0000-0002-7804-8130 (B.S.); 0000-0001-7609-0290 (C.S.).

Arbuscular mycorrhizas (AM) are the most common symbiotic associations between a plant's root compartment and fungi. They provide nutritional benefit (mostly inorganic phosphate [P_i]), leading to improved growth, and nonnutritional benefits, including defense responses to environmental cues throughout the host plant, which, in return, delivers carbohydrates to the symbiont. However, how transcriptional and metabolic changes occurring in leaves of AM plants differ from those induced by P_i fertilization is poorly understood. We investigated systemic changes in the leaves of mycorrhized *Medicago truncatula* in conditions with no improved P_i status and compared them with those induced by high-P_i treatment in nonmycorrhized plants. Microarray-based genome-wide profiling indicated up-regulation by mycorrhization of genes involved in flavonoid, terpenoid, jasmonic acid (JA), and abscisic acid (ABA) biosynthesis as well as enhanced expression of *MYC2*, the master regulator of JA-dependent responses. Accordingly, total anthocyanins and flavonoids increased, and most flavonoid species were enriched in AM leaves. Both the AM and P_i treatments corepressed iron homeostasis genes, resulting in lower levels of available iron in leaves. In addition, higher levels of cytokinins were found in leaves of AM- and P_i-treated plants, whereas the level of ABA was increased specifically in AM leaves. Foliar treatment of nonmycorrhized plants with either ABA or JA induced the up-regulation of *MYC2*, but only JA also induced the up-regulation of flavonoid and terpenoid biosynthetic genes. Based on these results, we propose that mycorrhization and P_i fertilization share cytokinin-mediated improved shoot growth, whereas enhanced ABA biosynthesis and JA-regulated flavonoid and terpenoid biosynthesis in leaves are specific to mycorrhization.

Arbuscular mycorrhizal (AM) fungi colonize the root system of over 80% of land plants through the development of an extensive hyphal network. AM fungi predominantly belong to the phylum Glomeromycota (Gehrig et al., 1996; Schussler et al., 2001). They enhance water uptake and mineral nutrition (mostly inorganic phosphate [P_i]) of the host plant, which, in return, provides photosynthates to the fungus through hyphal structures called arbuscules (Baier et al., 2010; Doidy et al., 2012). The major advantage to plants is enhanced biomass production in a P_i-limiting environment (Rooney et al., 2009; Adolfsson et al., 2015), although some studies reported a lack of positive effects on biomass or P_i status in AM plants (Smith et al., 2011; Schweiger et al., 2014b). Moreover, AM fungi provide nonnutritional benefits to the host, including resistance against pathogens and pests as well as tolerance to abiotic stress (Nadeem et al., 2014). These benefits make mycorrhization an attractive alternative to the use of costly fertilizers and harmful pesticides, which are incompatible with environmentally and economically sustainable development.

Phosphorous is a critical element for plant growth. P_i is the form taken up by the plant from the soil, where it can be poorly available owing to its low concentration and/or to its low solubility when bound to iron, aluminum, or calcium (Schachtman et al., 1998). This situation can be overcome by the interaction between the plant's root system and AM fungi, which accommodate an effective pathway, alternative to the direct root-epidermis uptake, by which soil P_i is absorbed in large amounts by the fungus and delivered to root cortical cells (Smith et al., 2011). However, some studies have suggested that the contribution of the AM-related P_i uptake pathway can be hidden due to the repression of

direct uptake (Smith et al., 2004; Schnepf et al., 2008). In these cases, subsequent changes in AM plants cannot be attributed entirely to an improved P_i content.

During the beginning of the last decade, pioneer transcriptomic studies revealed significant hints of the molecular basis of changes induced in mycorrhized roots. Changes were reported in the pathways related to cell wall modification, protein degradation, plant defense, and primary, secondary, and hormone metabolism in mycorrhized roots of *Medicago truncatula* (Journet et al., 2002; Liu et al., 2003; Hohnjec et al., 2005; Siciliano et al., 2007; Schliemann et al., 2008), *Oryza sativa* (Güimil et al., 2005), *Lotus japonicas* (Deguchi et al., 2007; Guether et al., 2009), and tomato (*Solanum lycopersicum*; Fiorilli et al., 2009; López-Ráez et al., 2010). The alterations in various types of metabolism are important for the establishment of the symbiosis and/or of interest for either of the partners, as exemplified below. Plant-synthesized sugars are transported to roots and supplied to the fungal symbiont. Flavonoids are thought to stimulate hyphal growth and branching (Scervino et al., 2005). Similarly, oxylipins regulate AM colonization and development (Isayenkov et al., 2005; Stumpe et al., 2005; León Morcillo et al., 2012). Finally, the coordinated action of auxins and strigolactones impacts root architecture (Cheng et al., 2013), whereas abscisic acid (ABA), jasmonic acid (JA), and salicylic acid (SA) are well known for priming tolerance to biotic and abiotic stress (Luo et al., 2009; Song et al., 2014).

Although AM symbiosis is restricted to the root, alterations also occur in the shoot, suggesting the existence of signaling pathways responsible for the induction of systemic responses throughout the plant (Cameron et al., 2013). Hormones involved in plant growth (auxins, cytokinins [CKs], and strigolactones) and in stress responses (ethylene, ABA, JA, and SA) are signals thought to mediate alterations in the roots as well as in the shoots of AM plants (Miransari et al., 2014).

M. truncatula is a well-established model plant for legume genomics (Cook, 1999). It has been broadly used for studies of transcriptomic, proteomic, and metabolomic changes induced by AM symbiosis in either roots or leaves (Liu et al., 2007; Schliemann et al., 2008; Abdallah et al., 2014; Schweiger et al., 2014b; Daher et al., 2017). Previous microarray-based transcriptional analyses in leaves of *M. truncatula* during AM symbiosis revealed systemic induction of genes involved in plant defense (Liu et al., 2007). Phenolic compounds such as flavonoids and triterpenoids of the saponin type are well-known major groups of secondary metabolites in leaves of *M. truncatula* (Gholami et al., 2014), but it is not clear how their production is affected by mycorrhization. Furthermore, AM-induced changes in secondary metabolism that are not driven by improved P_i status have not been investigated in *M. truncatula*.

In this study, we undertook a combination of microarray-based gene expression, metabolomic, and hormone analyses in leaves of *M. truncatula* plants in symbiosis with the AM fungus *Rhizophagus irregularis* and compared the observed alterations with those in P_i-treated nonmycorrhized plants. Using previously established conditions (Adolfsson et al., 2015), we could distinguish the specific effects of mycorrhization (i.e. not driven by P_i status) from those of P_i fertilization. We show that changes in secondary metabolites in leaves of AM plants correlate with the transcriptional regulation of related biosynthetic pathways. These modifications coincide with the specific modulation by mycorrhization of ABA biosynthesis and JA-regulated secondary metabolism. As common modifications of mycorrhization and P_i fertilization in leaves, we found the down-regulation of iron homeostasis genes and enhanced production of CKs, resulting in improved shoot growth.

RESULTS

Experimental Design to Dissect the Effects of Mycorrhization and P_i Fertilization

In this work, we cultivated *M. truncatula* with fungal inoculum (AM plants), mock inoculum (control plants), or mock inoculum treated with 5 mM P_i (P_i plants) under

[1] This work was funded by the Carl Tryggers Foundation, the Swedish Research Council, the Foundation Olle Engkvist Byggmästare, the Adlebertska Foundation, and the University of Gothenburg (C.S.), the Herbert and Karin Jacobsson Foundation and the Hvitfeldska Foundation (L.A.), the Ministry of Research and Education of the Republic of France and the University of Le Mans (B.S.), the Swedish Governmental Agency for Innovation Systems (VINNOVA) and the Swedish Research Council (K.L.). H.N. was the recipient of a postdoctoral fellowship from the Carl Tryggers Foundation. A.H. was the recipient of a postdoctoral fellowship from the Foundation Olle Engkvist Byggmästare. The metabolomics analysis was financed via a strategic grant from the Swedish University of Agricultural Sciences (T.M.). The plant hormone analysis was supported by the Ministry of Education, Youth, and Sport of the Czech Republic (the National Program for Sustainability I, grant no. LO1204) and the internal Grant Agency of Palacký University (IGA_PrF_2017_010; Ja.S., Ji.S., and O.N.).

[2] These authors contributed equally to the article.

[3] These authors contributed equally to the article.

[4] Address correspondence to cornelia.spetea.wiklund@bioenv.gu.se.

The author responsible for distribution of materials integral to the findings presented in this article in accordance with the policy described in the Instructions for Authors (www.plantphysiol.org) is: Cornelia Spetea (cornelia.spetea.wiklund@bioenv.gu.se).

L.A., H.N., B.S., and C.S. designed the experiments; T.M., O.N., K.L., and C.S. supervised the experiments; L.A. analyzed biomass and P_i content, estimated mycorrhization, prepared samples for microarray experiments, and analyzed the data sets; H.N. performed iron, anthocyanin, and flavonoid content analyses and contributed to analyses of microarray data sets; H.N., A.B., A.H., and J.A. performed quantitative RT-PCR; I.N.A. performed metabolomic analysis under the supervision of T.M.; Ja.S. and Ji.S. performed hormone analysis under the supervision of O.N. and K.L.; L.A. performed ANOVA statistical analysis on all data; H.N. and L.A. wrote the article with contributions from all the authors; C.S. supervised and complemented the writing.

[OPEN] Articles can be viewed without a subscription.

www.plantphysiol.org/cgi/doi/10.1104/pp.16.01509

previously established conditions (Adolfsson et al., 2015). Representative photographs of control, AM-, and P_i-treated plants are shown in Supplemental Figure S1 at 4 weeks post inoculation (wpi), when the degree of mycorrhization and the arbuscular abundance in AM plants were, on average, 72% and 51%, respectively (Table I; Supplemental Table S1). At this age, the AM symbiosis significantly increased shoot biomass as compared with the control without affecting the concentration of total P (expressed per shoot dry weight; Table I; Supplemental Table S1). In some experiments, we also included 1 mM P_i; however, this concentration appeared to be insufficient to induce a significantly high total P concentration in the shoot, whereas the biomass was only slightly higher than in control and AM plants (Supplemental Table S1), making it inappropriate to assess the effect of P_i fertilization. In 5 mM P_i-treated plants, the shoot total P concentration was significantly higher than in the control and AM plants (Table I; Supplemental Table S1), in agreement with our previous observations (Adolfsson et al., 2015). We also determined the concentration of soluble P (P_i) in shoots as well as in leaves and found that it followed a similar pattern to the total P (i.e. similar concentration in control and AM plants and significantly higher in the 5 mM P_i-treated plants; Supplemental Table S1). These experimental conditions allowed us to distinguish the specific effects of mycorrhization from those common with P_i fertilization in shoots of *M. truncatula*.

AM Symbiosis Induces Systemic Transcriptional Changes in Leaves Largely Different from P_i Fertilization

To advance our understanding of the molecular basis of AM-improved shoot growth, we carried out a microarray-based gene expression profiling in leaves from control, AM-, and P_i-treated *M. truncatula* plants at 4 wpi using a 60,000-feature oligonucleotide array. We considered to be significantly regulated only those genes showing a transcript ratio of treatment versus control with a threshold of 2 (Student's *t* test *P* value of 0.01 and false-positive error correction *Q* of 0.05), calculated using the false discovery rate method of Benjamin and Hochberg (1995). The RNA microarray data set from leaves of AM plants exhibited 297 significantly regulated genes as compared with the leaves of control plants (Fig. 1A). Among them, 183 genes were up-regulated (Supplemental Table S2), while 114 were down-regulated (Supplemental Table S3). A rough analysis of these genes revealed 143 whose predicted proteins are already annotated (http://plantgrn.noble.org/LegumeIP; Li et al., 2012). Through in silico searches in public databases using gene symbols (http://www.genome.jp/) and primary accession numbers (http://www.ncbi.nlm.nih.gov/unigene/) as well as through EST BLAST searching (https://blast.ncbi.nlm.nih.gov/Blast.cgi), we could assign a molecular function to predicted proteins of an additional 68 genes differentially regulated in AM leaves. A total of 86 genes encode proteins with either a yet uncharacterized function or without a known homolog and, therefore, were listed as unknown function/no homology. The most remarkable changes among AM-regulated genes were observed for those coding for a protein with unknown function (76-fold up-regulated; Supplemental Table S2) and for a vacuolar iron transporter/Nodulin-like protein (83-fold down-regulated; Supplemental Table S3). P_i treatment induced a significant transcript ratio (ratio > 2, $P < 0.01$, $Q < 0.05$) for 401 genes (Fig. 1A): 141 genes were up-regulated (Supplemental Table S4), whereas 260 genes displayed decreased transcript levels (Supplemental Table S5). The gene with the highest up-regulation (19-fold) encodes a mannitol transporter, whereas the strongest repressed (60-fold) was a P_i starvation-inducible gene.

When comparing gene expression profiles, 32 genes were found to be regulated by both AM symbiosis and P_i treatment, among which 21 were coregulated and 11 were conversely regulated (Fig. 1A; Supplemental Table S6). In each case, this represents about 5% of the total numbers of regulated genes in AM and P_i plants (297 and 401, respectively), suggesting that only a minor proportion of genes (and pathways) are affected by both treatments, whereas most genes (and pathways) altered by AM symbiosis are different from those altered by the P_i treatment.

Transcriptional Changes by AM Symbiosis and P_i Fertilization Involve Diverse Biological Processes

To get an overview of the functional relevance of transcriptional changes in leaves of AM and P_i plants, we conducted a functional process enrichment analysis

Table I. *Root mycorrhization, shoot dry weight, and total P concentration*

Parameter	Control	AM	P_i
Degree of mycorrhization (%)	0	72 ± 7	0
Arbuscular abundance (%)	0	51 ± 3	0
Shoot dry weight (g)	0.33 ± 0.04	0.50 ± 0.03*	0.60 ± 0.13**
Shoot total P (mg P g^{-1} dry weight)	1.5 ± 0.2	1.8 ± 0.3	13.2 ± 2.1***

M. truncatula plant material was harvested 4 wpi from control plants, plants infected with *R. irregularis* (AM), or plants treated with 5 mM P_i (P_i). Values are averages ± SD of three independent experiments, with four to six plants used in each experiment. Asterisks indicate significant differences between treatments and the control (one-way ANOVA, $P < 0.05$ [*], $P < 0.01$ [**], and $P < 0.001$ [***]; GraphPad Prism).

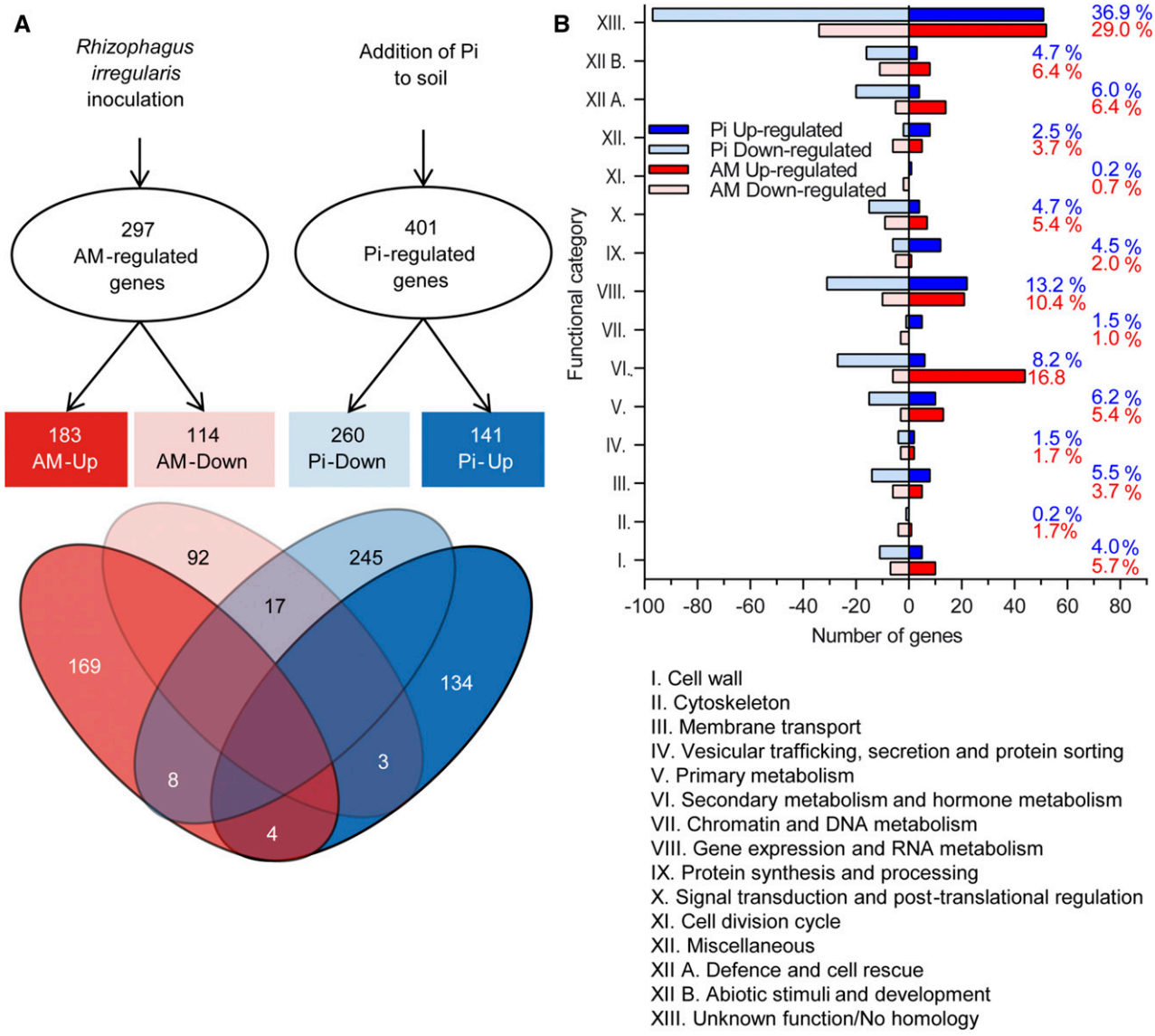

Figure 1. Overview of AM- and P_i-regulated genes in *M. truncatula* leaves. RNAs were extracted from leaves of *M. truncatula* plants inoculated with the fungus *R. irregularis* (AM) or fertilized with P_i. Significantly regulated genes have a transcript ratio of at least 2 and $Q < 0.05$ as compared with control plants. A, Venn diagram of common and specific genes regulated by AM and P_i treatments. B, Distribution of AM- and P_i-regulated genes into functional categories according to Journet et al. (2002). Values to the right in red and blue represent the proportion of genes in each functional category for AM and P_i treatment, respectively.

through manual inspection and annotation of putative proteins according to Journet et al. (2002). Fifteen functional classes were identified within both sets of AM- and P_i-regulated genes, with the class of unknown function/no homology being the most represented (Fig. 1B). For genes coding for proteins with a known function, the most represented functional classes in AM plants stand for secondary and hormone metabolism (16.8%), gene expression and RNA metabolism (10.4%), primary metabolism (5.4%), and defense and cell rescue (6.4%). In leaves of P_i-treated plants, gene expression and RNA metabolism (13.2%), secondary and hormone metabolism (8.2%), membrane transport (3.7%), primary metabolism (6.2%), and defense and cell rescue (6%) are the most represented classes. Notably, shared classes such as primary, secondary, and hormone metabolism and defense and cell rescue were dominated by up-regulated genes in AM and repressed genes in P_i-treated plants (Fig. 1B).

To confirm the microarray results, we carried out a quantitative reverse transcription (RT)-PCR analysis of 14 genes selected from various functional categories using RNA samples from the same experiment as the microarray as well as from an independent experiment

(Supplemental Table S1). Overall, the results are in good agreement with the microarray-based gene expression analysis (Supplemental Table S7).

AM Symbiosis and P_i Fertilization Differently Regulate Genes Involved in the Biosynthesis of Phenylpropanoid Derivatives

From the list of up- and down-regulated genes in AM plants (Supplemental Tables S2 and S3), we selected genes belonging to the same metabolic pathway. One of the most represented was phenylpropanoid biosynthesis, with enzymes coded by 10 AM-up-regulated genes (Table II). 4-Coumarate-CoA ligase5-like (4CL) is involved in early steps of this pathway, whereas dihydroflavonol reductase (DFR) and leucoanthocyanidin dioxygenase (LDOX; also called anthocyanidin synthase) are key enzymes in later steps of this pathway, yielding anthocyanins (Gholami et al., 2014). The other seven enzymes, namely caffeate 3-*O*-methyltransferase, isoflavonoid glycosyltransferase, isoflavonoid malonyl transferase, isoliquiritigenin 2′-*O*-methyltransferase, also called chalcone *O*-methyltransferase (CHMT), anthocyanidin 3-*O*-glucosyltransferase, anthocyanin 3′-*O*-β-glucosyltransferase (3′GT), and anthocyanin 5-aromatic acyltransferase, are implicated in the qualitative modification of phenylpropanoids (glycosylation and methylation), resulting in anthocyanins, isoflavonoids, flavones, and ferulates (Jaakola, 2013).

Among the genes of the phenylpropanoid biosynthetic pathway found to be up-regulated by AM symbiosis, *4CL* and *LDOX* were significantly down-regulated by P_i treatment (Table II). In addition, no change by mycorrhization but down-regulation by P_i was observed for the genes coding for cinnamoyl CoA reductase and cinnamyl alcohol dehydrogenase, involved in early steps of the phenylpropanoid pathway, and TRANSPARENT TESTA5/chalcone isomerase, involved in flavonoid biosynthesis (Supplemental Table S5; Gholami et al., 2014). In contrast, a gene coding for flavanol synthase/flavanone 3-hydroxylase, responsible for the biosynthesis of flavanols, was specifically up-regulated by P_i (Supplemental Table S4). *TRANSPARENT TESTA GLABRA2* (Nesi et al., 2001), which encodes a WRKY transcription factor that influences the biosynthesis of proanthocyanidins (PAs) and their derivatives, was specifically down-regulated by AM symbiosis (Table II).

AM Symbiosis Up-Regulates Genes Involved in Terpenoid Biosynthesis

Table II lists nine genes of the terpenoid biosynthesis pathway that were found to be significantly up-regulated by mycorrhization but not affected by P_i fertilization. The 3-hydroxy-3-methylglutaryl-coenzyme A reductase (HMG-CoA reductase) is a rate-controlling enzyme catalyzing the conversion of HMG-CoA to mevalonate, one of the first steps in terpenoid biosynthesis. Other affected genes were *TERPENE SYNTHASE1*, coding for a sesquiterpene synthase (Gomez et al., 2005), and *SQUALENE EPOXIDASE3*, coding for an enzyme helping in the first oxygenation step in sterol biosynthesis (Chugh et al., 2003). β-Amyrin synthase is committed to the first step in the biosynthesis of saponins, which are glycosylated triterpenoids protecting plants against pathogens and pests (Morita et al., 2000; Suzuki et al., 2002; Thimmappa et al., 2014). In addition, we found three genes for cytochromes P450: CYP76A61 and CYP93E2 (β-amyrin hydrolase), catalyzing the formation of the nonhemolytic sapogenin soyasapogenol B (Soya_B), and CYP72a67v2, which is a putative β-amyrin oxidase (Fukushima et al., 2013). Finally, *UGT73K1* encodes a triterpene UDP-glucosyl transferase dedicated to linking a sugar moiety to the triterpene aglycones hederagenin and soyasapogenols B and E to produce saponins (Achnine et al., 2005).

AM Symbiosis Activates Genes Involved in Lipid and Hormone Biosynthesis

AM symbiosis up-regulated the expression of two lipid biosynthetic genes, namely *DIACYLGLYCEROL ACYLTRANSFERASE* (*DGAT*), which helps in the processing of diacylglycerol (DAG) to triacylglycerol, and *TRIACYLGLYCEROL LIPASE*, dedicated to the conversion back to DAG (Table II). In contrast, two genes coding for GDSL-motif esterase/lipase acting as lipid hydrolases were found to be down-regulated in AM leaves. P_i treatment also up-regulated DGAT but did not significantly alter any other gene involved in lipid metabolism.

We also observed an increase in transcripts of genes involved in the biosynthesis of JA and other oxylipins, including the JA precursor 12-oxo-phytodienoic acid (*OPDA*). Genes encoding 9- and 13-lipoxygenases (9-LOXs and 13-LOXs, depending on where the oxygenation takes place), allene oxide synthase (AOS) and allene oxide cyclase (AOC), which successively convert the α-linolenic acid to OPDA, were all found to be up-regulated in leaves of AM plants. Besides this, the *MYC2* gene, known as a key positive regulator of JA signaling (Kazan and Manners, 2013), and two genes encoding jasmonate zim-domain (JAZ) proteins, acting as negative regulators of JA signaling, also were up-regulated (Table II). Furthermore, the gene coding for the homeobox-Leu zipper ATHB-7 as well as two isoforms of zeaxanthin epoxidases and 9-cis-epoxy-carotenoid dioxygenase, involved in ABA biosynthesis (Xiong and Zhu, 2003), were found to be up-regulated. Taken together, these results highlight the activation in AM leaves of oxylipin/JA- and ABA-regulated pathways, also known to promote systemic defense mechanisms in mycorrhized roots (Cameron et al., 2013). In addition, one gene coding for cytokinin-*O*-glucosyltransferase was up-regulated in AM leaves (Table II). Auxin- and ethylene-related genes were found to be either up- or down-regulated. In contrast to mycorrhization, P_i fertilization down-regulated the expression of *MYC2* and one *LOX* gene and did not

Table II. *List of selected altered genes in leaves of AM- and P_i-treated plants compared with controls*

Probe Set	Gene Identifier	Gene Name	AM Versus Control	*Q*	P_i Versus Control	*Q*
Phenylpropanoid biosynthesis						
A_27_P157881	MTR_3g087640	*Anthocyanin 5-aromatic acyltransferase*	**9.84**	0.019	−1.22	0.481
A_27_P066691	Mtr.24857	*Isoflavonoid glycosyltransferase*	**4.88**	0.005	−2.38	0.242
A_27_P073091	MTR_5g016660	*Anthocyanin 3′-O-β-glucosyltransferase (3′GT)*	**6.09**	0.015	−1.03	0.537
A_27_P071811	Mtr.17854	*Anthocyanidin 3-O-glucosyltransferase*	**3.39**	0.017	−1.96	0.227
A_27_P138561	MTR_4g090560	*Isoflavonoid malonyl transferase*	**2.04**	0.040	−1.18	0.407
A_27_P017915	MTR_3g031650	*Dihydroflavanol reductase (DFR)*	**2.03**	0.032	−1.46	0.209
A_27_P252062	MTR_7g011990	*Isoliquiritigenin 2′-O-methyltransferase (CHMT)*	**2.14**	0.032	−1.14	0.334
A_27_P262294	MTR_4g038440	*Caffeate 3-O-methyltransferase*	**2.09**	0.038	1.13	0.438
A_27_P041421	MTR_8g039720	*4-Coumarate-CoA ligase5-like (4CL)*	**2.73**	0.003	**−2.37**	0.016
A_27_P075601	MTR_3g070860	*Leucoanthocyanidin dioxygenase (LDOX)*	**2.55**	0.043	**−5.47**	0.006
A_27_P025011	MTR_7g100510	*Transparent testa glabra2 (TTG2)*	**−2.06**	0.017	−1.18	0.206
Terpenoid biosynthesis						
A_27_P071866	Mtr.6785	*Terpene synthase1*	**8.52**	0.007	−1.26	0.376
A_27_P095966	MTR_5g091050	*3-Hydroxy-3-methylglutaryl coenzyme A reductase (HMG-CoA reductase)*	**7.95**	0.049	−2.54	0.081
A_27_P319642	MTR_8g072640	*3-Hydroxy-3-methylglutaryl coenzyme A reductase (HMG-CoA reductase)*	**3.27**	0.039	−4.50	0.060
A_27_P249272	MTR_4g031800	*Triterpene UDP-glucosyl transferase (UGT73K1)*	**3.54**	0.050	−1.01	0.551
A_27_P060581	MTR_4g031820	*Cytochrome P450 monooxygenase (CYP72A61)*	**3.21**	0.009	−1.03	0.534
A_27_P280972	Mtr.3401	*Cytochrome P450 monooxygenase (CYP72a67v2)*	**3.19**	0.022	−4.91	0.110
A_27_P012095	MTR_4g005190	*β-Amyrin synthase*	**3.08**	0.023	−2.50	0.233
A_27_P060566	Mtr.15375	*Cytochrome P450 monooxygenase (CYP93E2)*	**2.82**	0.008	−1.71	0.180
A_27_P098361	NA	*Squalene epoxidase3 (SQE3)*	**2.81**	0.005	−1.44	0.069
Lipid biosynthesis, metabolism, and transfer						
A_27_P099341	MTR_5g017260	*Triacylglycerol lipase*	**3.70**	0.002	−1.63	0.166
A_27_P248717	MTR_4g124080	*Diacylglycerol acyltransferase (DGAT)*	**2.87**	0.050	**3.51**	0.001
A_27_P084651	MTR_7g087190	*GDSL-motif esterase/lipase*	**−3.49**	0.050	1.46	0.141
A_27_P355817	NA	*GDSL-motif esterase/lipase*	**−2.77**	0.045	−2.28	0.066
Oxylipin/JA signaling						
A_27_P258482	MTR_5g013530	*Jasmonate zim-domain (JAZ) protein*	**5.44**	0.004	1.13	0.506
A_27_P238868	MTR_5g024020	*9S-Lipoxygenase (9-LOX)*	**4.66**	0.006	−1.69	0.273
A_27_P062321	MTR_8g018730	*9S-Lipoxygenase (9-LOX)*	**4.29**	0.003	−1.47	0.327
A_27_P110056	MTR_8g107300	*Jasmonate zim-domain (JAZ) protein*	**3.41**	0.033	2.23	0.338
A_27_P057826	MTR_8g067280	*MYC2 transcription factor*	**3.38**	0.032	**−3.51**	0.025
A_27_P330397	MTR_5g053950	*Allene oxide cyclase (AOC)*	**3.05**	0.019	−1.34	0.257
A_27_P097056	NA	*13S-Lipoxygenase, similar to AtLOX2*	**2.84**	0.020	−1.39	0.337
A_27_P091546	Mtr.22358	*9S-Lipoxygenase*	**2.32**	0.032	−1.77	0.173
A_27_P344712	NA	*13S-Lipoxygenase, similar to AtLOX2*	**2.25**	0.049	−1.57	0.284
A_27_P094741	NA	*Lipoxygenase5 (LOX5)*	**2.18**	0.034	−2.56	0.065
A_27_P013630	MTR_4g068550	*Allene oxide synthase (AOS)*	**2.01**	0.025	−1.11	0.415
ABA						
A_27_P320287	NA	*9-cis-Epoxycarotenoid dioxygenase*	**3.76**	0.005	−1.19	0.406
A_27_P243492	NA	*Zeaxanthin epoxidase*	**3.65**	0.000	1.17	0.333
A_27_P258127	MTR_5g017330	*Zeaxanthin epoxidase*	**2.22**	0.003	1.11	0.260
A_27_P047556	MTR_8g026960	*Homeobox-Leu zipper protein ATHB-7*	**2.16**	0.039	1.39	0.266

(*Table continues on following page.*)

Table II. (*Continued from previous page.*)

Probe Set	Gene Identifier	Gene Name	AM Versus Control	*Q*	P_i Versus Control	*Q*
Ethylene						
A_27_P047216	Mtr.12275	*1-Aminocyclopropane-1-carboxylate oxidase*	**2.48**	0.035	−1.62	0.240
A_27_P074801	MTR_2g025120	*1-Aminocyclopropane-1-carboxylate oxidase*	**−2.51**	0.032	1.63	0.324
A_27_P009606	MTR_7g020980	*Ethylene-responsive transcription factor*	**−2.94**	0.035	−2.16	0.058
CK						
A_27_P005847	MTR_2g035020	*Cytokinin-O-glucosyltransferase*	**3.51**	0.032	−1.23	0.467
Auxin						
A_27_P199111	MTR_5g005670	*Trp synthase β-chain*	**2.12**	0.030	1.72	0.010
A_27_P287213	MTR_104s0003	*Auxin-responsive AUX/IAA-gene family member*	**−2.34**	0.010	1.26	0.120
Iron homeostasis						
A_27_P065276	MTR_5g083170	*Ferritin2* (*FER2*)	**−3.03**	0.032	**−2.32**	0.037
A_27_P065856	MTR_4g014540	*Ferritin3* (*FER3*)	**−6.30**	0.015	**−4.92**	0.006
A_27_P249542	MTR_1g099010	*Vacuolar iron transporter/Nodulin-like protein* (*VIT*)	**−6.74**	0.022	−2.18	0.065
A_27_P326777	MTR_7g069980	*Ferritin1* (*FER1*)	**−35.53**	0.003	**−21.61**	0.001
A_27_P311167	MTR_6g034975	*Vacuolar iron transporter/Nodulin-like protein* (*VIT*)	**−83.29**	0.007	**−10.26**	0.002

Values in boldface represent significant alterations in AM or P_i plants versus controls (transcript ratio of at least 2, $Q < 0.05$). Positive and negative ratios indicate up- and down-regulated genes, respectively. NA, Not annotated. Complete data sets for alteration in gene expression are presented in Supplemental Tables S2 to S5.

significantly alter any other genes involved in hormone biosynthesis or signaling (Table II).

AM Symbiosis and P_i Fertilization Down-Regulate Genes Involved in Iron Homeostasis

Iron (Fe) is an essential mineral nutrient for plants and serves as a cofactor for enzymes involved in respiration, chlorophyll biosynthesis, and chloroplast development (Nishio et al., 1985; Kobayashi and Nishizawa, 2012). However, excess free Fe(II) is toxic for cells due to the formation of hydroxyl radicals, causing deleterious effects to cellular constituents (Orino et al., 2001). Well-known Fe homeostasis genes were found to be down-regulated in leaves of both AM- and P_i-treated plants (Table II). These include genes coding for FERRITIN1 (FER1), FER2, and FER3, which serve in the storage of Fe (Arosio et al., 2009), and two vacuolar iron transporters (VITs) whose Arabidopsis (*Arabidopsis thaliana*) counterpart promotes the influx of Fe into vacuoles (Kim et al., 2006).

AM Symbiosis and P_i Fertilization Decrease Total Iron, Whereas AM Specifically Increases Flavonoid and Anthocyanin Contents

Because Fe homeostasis genes were down-regulated by AM and P_i, we assumed that leaf Fe content was altered by these treatments. To verify this hypothesis, we used the Ferrozine-based assay (Stookey, 1970) and determined available Fe(II) and Fe(III), two stable and interconvertible forms of Fe. As expected, both Fe(II) and Fe(III) levels were lower in AM and P_i plants as compared with control plants (Fig. 2A), suggesting that the down-regulation of Fe homeostasis genes might be the consequence of the reduction in available Fe.

Next, we verified whether transcriptional changes of phenylpropanoid-related genes impacted flavonoid and anthocyanin contents in leaves. As expected, both contents were increased significantly in AM plants, while those of P_i-treated plants were unchanged compared with control plants (Fig. 2, B and C), in line with the up-regulation by mycorrhization of genes involved in flavonoid and anthocyanin biosynthesis (Table II).

AM Symbiosis Regulates the Levels of Phenylpropanoid, Lipids, and Terpenoid Metabolites

To get information about metabolite changes in AM leaves as compared with 5 mM P_i-treated and control leaves, we carried out an untargeted metabolomic analysis at 4 wpi. With the purpose of testing our experimental setup for this type of analysis, we also included in this experiment plants treated with 1 mM P_i, knowing that they display nonsignificantly different P concentrations in leaves from control and AM plants (Supplemental Table S1). From the metabolite profile (Supplemental Table S8), an orthogonal partial least

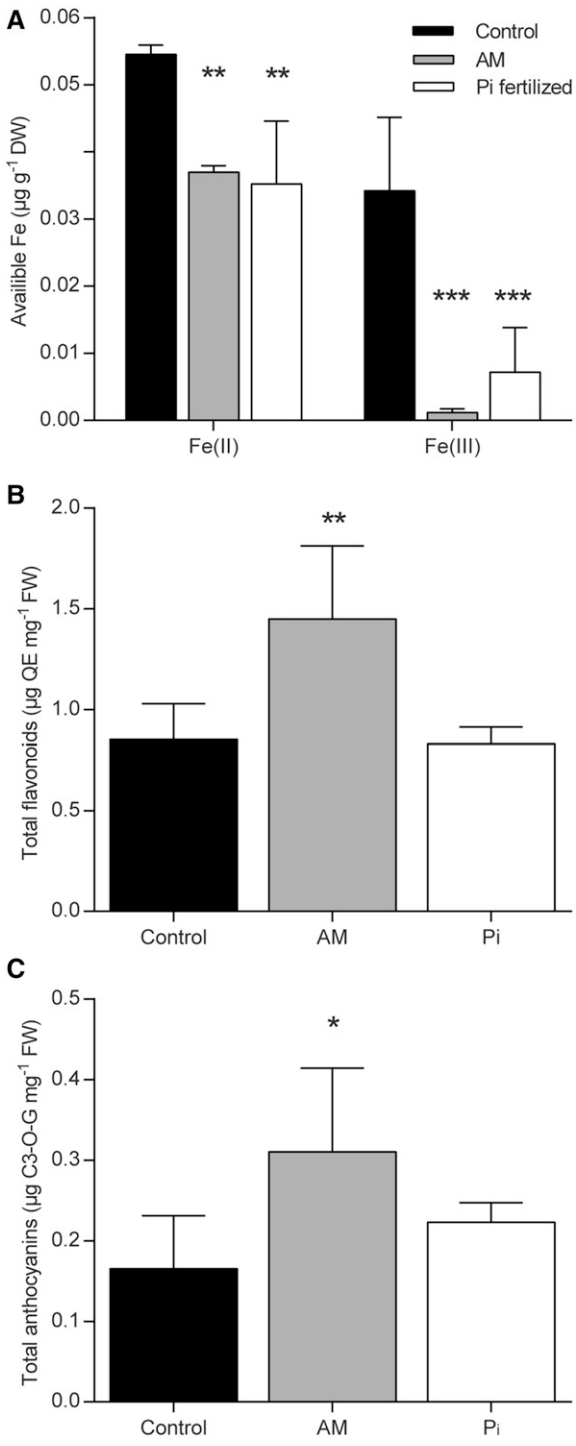

Figure 2. Quantification of available Fe, total flavonoids, and anthocyanins in *M. truncatula* leaves. A, Content of (Fe)II and Fe(III). B, Total flavonoids expressed as quercetin equivalent (QE). C, Total anthocyanins expressed as cyanindin 3-*O*-glucoside equivalent (C3-O-G). Bars represent means ± SD from four plants. Asterisks indicate significant differences between treatments and the control (one-way ANOVA, $P < 0.05$ [*], $P < 0.01$ [**], and $P < 0.001$ [***]; GraphPad Prism). DW, Dry weight; FW, fresh weight.

squares discriminant analysis (OPLS-DA; Trygg and Wold, 2002) was performed, and individual comparison was performed between the control and the AM or the two P_i treatments (Supplemental Fig. S2A). Indeed, no valid statistical models could discriminate between the profiles of control and 1 mM P_i treatment. The SUS (Shared and Unique Structures) plot (see "Materials and Methods") between the two valid statistical models was used to select similar metabolite trends between 5 mM P_i-treated and AM leaves. Student's *t* test was performed between control × 5 mM P_i and control × AM plants, and multiple testing correction was performed according to Benjamin and Hochberg (1995; Supplemental Table S9). Metabolites displaying significant differences ($Q < 0.05$) are listed in Table III. We discovered that major changes in leaves from AM plants compared with control plants fell mainly into the categories of phenylpropanoid derivatives (flavonoids and other phenylpropanoids), carotenoid derivatives, glycerolipids, saponin-type terpenoids, and glucoside conjugates.

Among flavonoids, the levels of proanthodelphinidin, a luteolin derivative, and the isoflavonoid fromosin-7-*O*-glucoside-6′′-*O*-malonate were increased in AM leaves, contrasting with the decreased levels of prenylchalcone and an apigenin glucoside. Furthermore, the levels of other phenylpropanoid-conjugated forms either decreased (ferulates) or increased (glycosylates) in AM plants, whereas two ferulates also decreased in P_i-treated plants.

Blumenol B malonylglucoside, dihydroxyphaseic acid-like, and tributyrin glucoside decreased in leaves of AM plants. Surprisingly, a metabolite tentatively annotated as dihydroxy blumenol glucoside (Supplemental Fig. S3) decreased about 30,000-fold in AM plants. Galactolipids (mono and diacyl forms) were enhanced in AM plants, whereas the saponin derivatives and several glucoside conjugates responded in different ways in AM plants. No saponins or glucoside conjugates were affected in leaves of P_i-treated plants, but 2-benzyl succinate was found to be down-regulated.

AM Symbiosis and P_i Fertilization Stimulate the Production of CKs, Whereas AM Specifically Stimulates ABA Production

The plant hormones CKs and auxins are the main players in leaf development and nutrient allocation (Spíchal, 2012; Vanstraelen and Benková, 2012), whereas SA, JAs, and ABA are well known for their roles in plant responses to biotic and abiotic stresses (Rivas-San Vicente and Plasencia, 2011; Finkelstein, 2013; Yan et al., 2013). Therefore, we expected that the influence of AM symbiosis on host metabolism also would be reflected in the hormonal composition and levels when compared with control plants. Highly sensitive methods utilizing mass spectrometry were used for the detection of compounds from CKs, auxins, JAs, ABA, and SA families (Novák et al., 2012; Svačinová et al., 2012; Floková et al., 2014).

Table III. *List of metabolites increased or decreased in leaves of AM- and P_i-treated plants compared with controls*

m/z	Retention Time	Metabolite Class	AM Versus Control	*Q*	P_i Versus Control	*Q*
	min					
Flavonoids						
355.1	1.848	Prenylchalcone	**−1.89**	0.000	−1.17	0.442
353.1	1.909	Prenylchalcone	**−1.93**	0.000	−1.21	0.383
613.2	1.249	Proanthodelphinidin	**2.09**	0.027	1.35	0.725
575.2	3.030	Fromosin-7-*O*-glucoside-6′′-*O*-malonate	**1.35**	0.026	1.20	0.554
575.2	3.181	Fromosin-7-*O*-glucoside-6′′-*O*-malonate	**1.23**	0.027	1.16	0.561
649.3	3.394	Apigenin glucuronic glucoside	**−3.23**	0.026	−2.41	0.205
991.2	3.598	Luteolin glucuronic 5OH-coniferyl alcohol	**1.59**	0.028	1.37	0.776
Other phenylpropanoids						
344.1	2.702	Coumaroyl-glucoside	**1.55**	0.028	1.58	0.117
439.2	2.797	1′-*O*-Benzyl-L-rhamnopyranosyl	**1.35**	0.039	1.12	0.762
439.2	3.050	1′-*O*-Benzyl-L-rhamnopyranosyl	**−1.53**	0.026	−1.18	0.115
476.2	3.450	*N*-Feruloyltyramine glucoside	**−1.59**	0.008	−1.15	0.130
353.1	3.174	Ferulic acid-GlcA	**−0.70**	0.011	**−1.71**	0.012
445.1	3.174	Ferulic acid-GlyA-glycerol	**−1.69**	0.011	**−1.74**	0.012
314.1	3.451	*N*-Feruloyltyramine	**−1.57**	0.022	−1.17	0.113
314.1	3.940	*N*-Feruloyltyramine	**−1.70**	0.009	−1.17	0.352
561.2	3.170	Dilignol glucoside	**1.21**	0.020	1.33	0.227
Carotenoid derivatives and lipids						
433.2	4.298	Dihydroxy blumenol glucoside	**−30,090**	0.000	1.28	0.332
465.2	4.198	Blumenol B malonylglucoside	**−2.17**	0.001	−1.97	0.101
285.2	3.566	Dihydroxyphaseic acid-like	**−3.07**	0.028	−2.30	0.117
487.2	3.479	Tributyrin glucoside (triacylglycerol)	**−3.11**	0.028	−1.95	0.131
537.3	6.021	MGMG (18:3)	**1.97**	0.027	1.79	0.306
799.5	7.715	MGDG (36:5)	**1.40**	0.042	1.38	0.401
Saponins						
1383.6	4.420	Medicagenic acid derived	**1.29**	0.044	1.43	0.115
1385.6	4.088	Zhanic acid derived	**1.38**	0.031	1.23	0.612
1564.7	4.098	3-Glc-Glc-Glc, 23-Ara, 28-Ara-Rha-Xyl zhanic acid	**1.73**	0.005	1.33	0.621
1254.6	4.192	Hederagenin derived	**−1.37**	0.009	1.04	0.630
953.5	4.225	Oleanolic acid derived	**−1.48**	0.014	−1.05	0.437
957.5	4.690	dHex-Hex-HexA-Hederagenin	**−2.13**	0.011	−1.49	0.101
1117.5	4.732	Hederagenin derived	**−2.27**	0.022	−1.55	0.323
999.5	5.200	Soya_B derived	**−2.46**	0.024	−1.54	0.115
1029.5	5.202	Soya_B derived	**−2.24**	0.045	−1.47	0.115
867.5	5.203	Soya_B derived	**−2.54**	0.025	−1.66	0.115
1011.5	5.218	Soya_B derived	**−2.12**	0.037	−1.48	0.118
1029.5	5.447	Soya_B derived	**−2.37**	0.041	−1.69	0.115
1131.6	5.235	Sophoradiol derived	**−2.34**	0.032	−1.45	0.182
Glucoside conjugates						
342.1	1.599	6-(α-D-Glucosaminyl)-1D-myoinositol	**1.19**	0.032	1.05	0.721
289.2	3.747	1-*O*-Hexyl-D-glucitol	**1.23**	0.006	1.33	0.127
361.1	1.821	Syringaldazine	**1.39**	0.020	1.21	0.700
267.2	3.116	1-*O*-Hexyl-D-Mannitol	**−1.26**	0.028	1.00	0.628
223.2	2.916	2-Benzyl-2-hydroxybutanedioate	**−1.38**	0.000	1.10	0.428
317.1	2.676	Glc-L-rhodinose	**−1.36**	0.014	−1.28	0.205
207.1	3.181	2-Benzylsuccinate	−1.72	0.089	**−1.36**	0.023

Values marked in boldface represent significant alterations presented as metabolite ratios in AM or P_i plants versus controls ($Q < 0.05$). Positive and negative ratios indicate increased and decreased levels, respectively. The values presented are based on peak area normalized against leaf fresh weight and are means of seven to eight plants. *m/z* is the mass-to-charge ratio of the molecular ion. Complete data sets of metabolites are presented in Supplemental Tables S8 and S9.

Thirty compounds from targeted plant hormone families were detected (Supplemental Table S10), quantified, and statistically evaluated in leaf samples from the control, AM-, and P_i-fertilized plants. A principal component analysis (PCA) plot shows clear separation of all groups and clustering of samples of the same group (Fig. 3A). From OPLS-DA S-plots, hormones with the highest correlation and covariance were selected (top right corner and bottom left corner of the S-plot; Supplemental Fig. S4). When comparing AM treatment versus control, cytokinin species (dihydrozeatin [DHZ], trans-zeatin riboside [tZR], trans-zeatin 9-glucoside

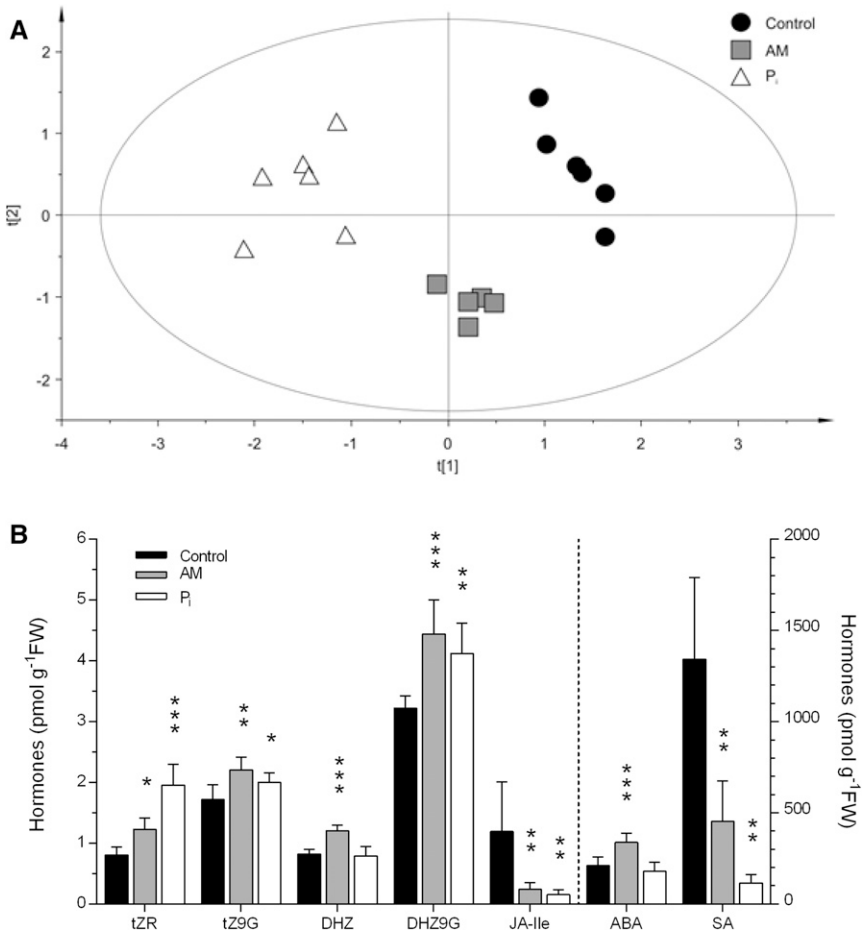

Figure 3. Quantification of hormones in *M. truncatula* leaves. A, PCA score plot (explained variance $R^2 = 0.722$ and predicted variance $Q^2 = 0.0801$; ellipse, Hotelling's T2 [95%]). B, Content of cytokinin species (tZR, trans-zeatin riboside; tZ9G, trans-zeatin 9-glucoside; DHZ, dihydrozeatin; DHZ9G, dihydrozeatin 9-glucoside) and the stress-related hormones JA-Ile, ABA, and SA. Bars represent means ± SD from six plants. Asterisks indicate significant differences between treatments and the control (one-way ANOVA, $P < 0.05$ [*], $P < 0.01$ [**], and $P < 0.001$ [***]; GraphPad Prism). FW, Fresh weight.

[tZ9G], dihydrozeatin 9-glucoside [DHZ9G], trans-zeatin [tZ], and dihydrozeatin riboside [DHZR]) and ABA (increased concentrations in AM) and SA and JA-Ile (decreased concentrations in AM) can be selected (Supplemental Fig. S4A). When comparing P_i treatment versus control, tZR and DHZ9G (increased concentrations in P_i) and SA and JA-Ile (decreased concentrations in Pi) can be selected (Supplemental Fig. S4B). Further statistical analysis of selected metabolites with ANOVA followed by Fisher's LSD test for multiple comparisons highlights that ABA and the CK metabolite DHZ were increased specifically in AM leaves, whereas the other hormone species were altered similarly by mycorrhization and P_i fertilization (Fig. 3B).

JA But Not ABA Application Activates Genes Involved in Flavonoid and Terpenoid Biosynthesis

The up-regulation of genes involved in ABA biosynthesis (Table II) coincided with the enhanced level of ABA specifically in leaves of AM plants (Fig. 3B). Based on the up-regulation of genes involved in JA biosynthesis (Table II), we also expected an enhanced level for this hormone in AM plants. Since this was not confirmed by our measurements (Fig. 3B), we hypothesized that JAs might have increased initially in AM leaves and, thereafter, were transported toward distal tissues such as roots, resulting in a reduced steady-state level of JAs in leaves. Alternatively, increased JAs could be present in leaves in forms not detectable by the method used. Furthermore, genes involved in ABA and JA signaling as well as genes involved in phenylpropanoid and terpenoid biosynthesis were up-regulated specifically in leaves of AM plants (Table II).

To investigate whether increased ABA and JA levels in leaves can affect secondary metabolism, we analyzed the expression of involved genes in nonmycorrhized plants whose leaves were treated with either methyl jasmonate (MeJA) or ABA at two concentrations. After 24 h of treatment at the higher concentrations (1 mM MeJA and 100 μM ABA), the expression of *ATHB-7*, used as a positive control for ABA-responsive genes, was indeed enhanced significantly in leaves by ABA but not by MeJA application as compared with leaves of control-treated plants (Fig. 4). The expression of *MYC2*, the master regulator of JA signaling, was significantly and similarly enhanced by 1 mM MeJA and 100 μM ABA. The expression of AM-regulated genes involved in JA biosynthesis (*AOS*) and signaling (*JAZ*/MTR_5g013530), in the production of flavonoids (*LDOX* and *3′GT*), and in the biosynthesis of saponin-type terpenoids (*UGT73K1*) was significantly up-regulated by MeJA but not by ABA

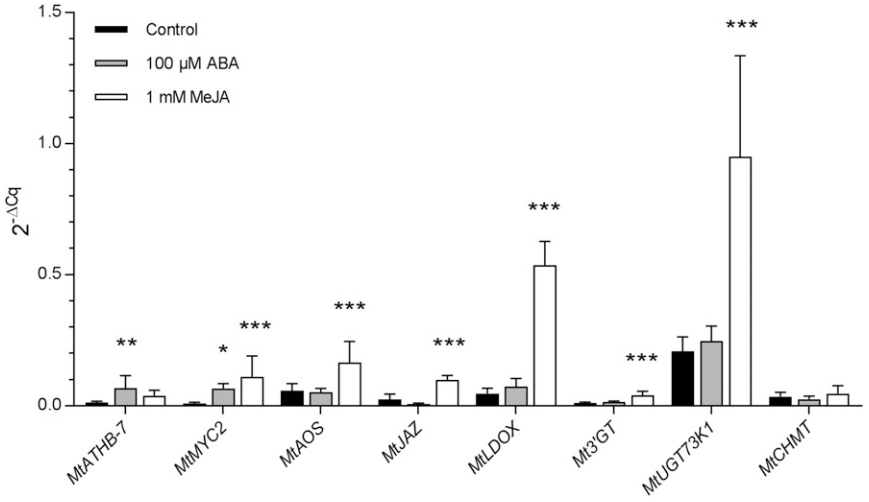

Figure 4. Relative expression of genes involved in flavonoid biosynthesis in leaves of nonmycorrhized *M. truncatula* plants in response to 100 μM ABA and 1 mM MeJA treatments. Total RNA was isolated after 24 h of treatment, and changes in transcript abundance were determined by quantitative RT-PCR analysis. The relative expression of *MtATHB-7* (MTR_8g026960), *MtMYC2* (MTR_8g067280), *MtAOS* (MTR_4g068550), *MtJAZ* (MTR_5g013530), *MtLDOX* (MTR_3g070860), *Mt3′GT* (MTR_5g016660), *MtUGT73K1* (MTR_4g031800), and *MtCHMT* (MTR_7g011990) genes was calculated as $2^{-\Delta Cq}$ and normalized using *MtTef-1a* as an internal reference gene. Bars represent means ± SD from six plants. Asterisks indicate significant differences between treatments and the control (one-way ANOVA, $P < 0.05$ [*], $P < 0.01$ [**], and $P < 0.001$ [***]; GraphPad Prism).

treatment of leaves. Interestingly, expression of the *CHMT* gene, which is involved in the methylation of isoflavonoids, was not found to be altered by either MeJA or ABA application. This observation, together with the fact that the expression of this gene was found to be up-regulated by AM symbiosis (Table II), suggests that factors other than ABA and JAs may be involved in isoflavonoid production. The lower concentrations of hormones (100 μM MeJA and 10 μM ABA) were not sufficient in our conditions to significantly alter the expression of the above AM-regulated genes (Supplemental Table S11). The insignificant expression change of *MYC2* by the lower concentration of MeJA could be explained by the fact that this is an early JA-induced gene (Ding et al., 2011; An et al., 2016), so that its expression levels may be down again at 24 h after the application of MeJA. Taken together, these data suggest that the treatment of leaves from nonmycorrhized plants with 1 mM MeJA can induce a similar pattern of alterations in JA biosynthesis and signaling pathways as well as flavonoid and terpenoid biosynthesis to that in AM plants, most likely via *MYC2*-regulated pathways. Although treatment with 100 μM ABA up-regulates *MYC2* expression, this does not activate either the JA pathways or the biosynthesis of flavonoids and terpenoids in leaves.

DISCUSSION

As compared with the knowledge available about transcriptomic and metabolomic changes in roots of mycorrhized *M. truncatula* plants, little attention has been paid to corresponding alterations occurring in shoots, their underlying cellular pathways, as well as their interconnections. In this study, we investigated the transcriptional regulation of the genome and metabolic changes in shoots of AM plants with similar P status to control plants and compared them with those induced by treatment with high P_i (5 mM) using a previously established experimental system (Adolfsson et al., 2015). Our choice of concentration for the P_i treatment arose from similar studies in legumes comparing control, AM, and P_i treatments. Schliemann et al. (2008) followed the kinetics of the accumulation of primary and secondary metabolites in *M. truncatula* and found distinct profiles for AM, nonmycorrhized, and 13.3 mM P_i-treated roots. Grunwald et al. (2009) studied transcriptional changes in control, AM- (three *Glomus* spp.), and P_i-fertilized (1.3 mM) *M. truncatula* roots containing 6-fold more P_i than the control. Hence, we assumed that fertilization with 5 mM P_i, yielding 7-fold more P_i than in control and AM plants, was an appropriate treatment in our experimental conditions to distinguish the AM-specific changes from those shared with P_i fertilization in *M. truncatula* leaves.

The microarray-based gene expression analysis revealed a minor overlap of transcriptional changes in leaves of AM- and P_i-fertilized plants (21 out of 297 genes; i.e. approximately 7%). A low overlap between AM- and high-P_i-induced gene expression also was reported for *M. truncatula* roots (4%; Hohnjec et al., 2005). This, together with our observations, strengthens the view that systemic transcriptional responses in leaves and roots of AM plants are largely due to mycorrhization and not shared with P_i fertilization. In line with the transcriptional pattern, OPLS-DA of the metabolomic analysis showed largely distinct metabolite profiles for AM- and P_i-treated plants (Supplemental Fig. S2A). Of

the secondary metabolites that were significantly different in AM leaves as compared with control leaves, only two out of 41 were altered in a similar manner in the P_i treatment (Table III). Some discordance observed between transcriptomic and metabolomic results could be explained by posttranslational modifications regulating the activity of enzymes as well as metabolite fluxes (Fernie and Stitt, 2012). A previous metabolomics study on *Plantago major* leaves under mycorrhization with *R. irregularis* (Schweiger et al., 2014a) found 40% of the AM metabolites (mostly primary metabolites) in P_i-treated plants, which was explained on the basis of similar P_i concentrations in leaves of the two treatments.

AM Symbiosis Regulates Flavonoid/Anthocyanin and Terpenoid Biosynthesis

The RNA microarray data sets from AM leaves revealed the up-regulation of several transcripts involved in the biosynthesis of phenylpropanoid derivatives, especially flavonoids including anthocyanins (Table II; Fig. 5A). Determination of the total anthocyanin and flavonoid contents also suggests an increase in the biosynthesis of phenolic metabolites compared with the control (Fig. 2, B and C).

Previous studies have shown changes in transcript levels of flavonoid biosynthetic genes in roots of *M. truncatula* infected with AM fungi (Wulf et al., 2003; Liu et al., 2007). In roots, flavonoids are believed to stimulate fungal spore germination and hyphal growth and branching (Scervino et al., 2005). In our study, we observed one luteolin glucoside and proanthodelphinidin (a subset of PAs) increased in leaves of mycorrhized plants, while prenylchalcone and an apigenin glucoside decreased (Fig. 5A; Table III). Similarly, an improvement of luteolin-7-*O*-glucoside was observed in shoots of mycorrhized willow (*Salix purpurea*; Aliferis et al., 2015).

The glycosylation of flavonoids is important for their stability and solubility during transport and storage

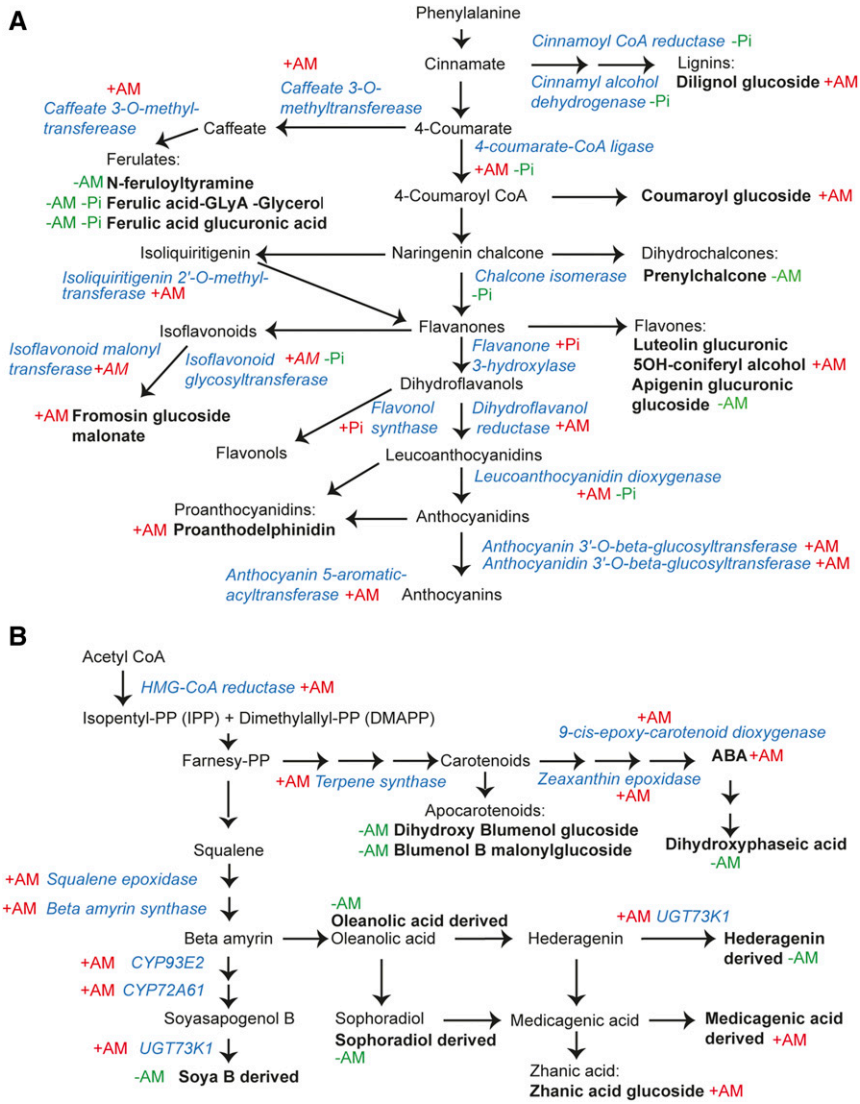

Figure 5. Scheme summarizing transcriptional regulation and metabolite changes. A, The phenylpropanoid biosynthetic pathway. B, The terpenoid and apocarotenoid biosynthetic pathway. Names of metabolites and their derivatives are written in black, whereas those of the enzymes involved are written in blue. Plus (+) and minus (−) in front of AM and/or P_i indicate increase or decrease, respectively, in expression of the corresponding genes or in metabolite levels.

into the vacuole (Jiang et al., 2008; Plaza et al., 2014). The conversion of anthocyanidin to anthocyanin is driven by glycosyltransferases, whose expression was found to be stimulated in leaves during AM symbiosis (Table II; Fig. 5A). Anthocyanins are known to protect plants from excess light and prevent oxidative stress; similarly, PAs, which are also antioxidants, are involved in plant protection against insects and pathogens (Mouradov and Spangenberg, 2014).

A significant number of genes from the terpenoid biosynthesis pathway were found to be up-regulated by mycorrhization (Fig. 5B). Although we observed an overall decrease in terpenoids, a glycosylated zhanic acid derivative was increased significantly in AM leaves compared with controls. This could be explained based on the reduction in hederagenin derivative, which might have favored zhanic acid production, a parallel branch in the terpenoid biosynthetic pathway (Fig. 5B). All these changes could reflect the notion that terpenoids have a wide range of basic functions in growth and also are involved in defense against abiotic and biotic stress (Tholl, 2015).

ABA is the most studied member of plant apocarotenoids, which are cleavage products from a C_{40} carotenoid precursor. The hormone and microarray analyses indicate correlation between the increased ABA levels and the up-regulation of related biosynthetic genes in leaves of AM plants (Fig. 5B). This does not exclude the possibility proposed by Cameron et al. (2013) that ABA synthesized in mycorrhized roots is transported and may act as a long-distance signal for defense responses in leaves. Furthermore, the metabolomic analysis indicates significant decreases in the apocarotenoids blumenol B malonyl glucoside and dihydroxyphaseic acid-like in leaves of AM plants. Intriguingly, a dihydroxy blumenol glucoside almost completely disappeared in AM leaves (Table III). Cyclic C_{13} cyclohexenone-/α-inono- (e.g. blumenol) glucosides as well as yellow linear C_{14} mycorradicines have been associated with the establishment of mycorrhiza in roots (Floss et al., 2008; Schliemann et al., 2008) and are suggested to play a role in arbuscule turnover (Walter et al., 2010). Both ABA and blumenol are derived from all-trans-lycopene (for review, see Hou et al., 2016). The strong reduction of the dihydroxy blumenol glucoside in mycorrhized leaves could be due to either competing biosynthesis with ABA (Fig. 5B) or the long-distance transport to mycorrhized roots.

AM Symbiosis and P_i Fertilization Modulate Iron Homeostasis

Well-known Fe homeostasis genes such as *VIT*, *FER1*, *FER2*, and *FER3* were remarkably down-regulated by AM symbiosis and P_i treatment (Table II). Repression of these genes correlated with the observed decrease of both Fe(II) and Fe(III) (Fig. 2A). It is worthy of note that an excess of available Fe(II) is toxic for cells due to the formation of hydroxyl radicals (Orino et al., 2001). To prevent this, cells orchestrate strategies to regulate Fe homeostasis by means of either oxidation of Fe(II) to Fe(III), the nontoxic form of Fe, chelation, sequestration by ferritins in plastids, or its transport into vacuoles through VIT (Arnaud et al., 2006; Ravet et al., 2009).

P_i acts as a strong chelator of Fe(II) (Rasmussen and Toftlund, 1986), so that a reduced available Fe content in leaves of P_i-treated plants was expected. Flavonoids also are well known as Fe chelators (Mira et al., 2002; Takeda, 2006). Hence, it is tempting to speculate that increased levels of flavonoids/anthocyanins/PAs in AM leaves favor Fe binding, thereby resulting in the down-regulation of Fe homeostasis genes. Because AM symbiosis also enhances flavonoid biosynthesis in the root (Harrison and Dixon, 1994; Larose et al., 2002), it is possible that flavonoids also modulate Fe homeostasis in this tissue, although contradictory results about the effect of mycorrhization on root Fe status were reported (Jin et al., 2014).

Increase of CKs May Promote Shoot Growth in AM- and P_i-Treated Plants

CKs are well-known signaling molecules promoting plant growth. Based on our data, increased levels of CKs in leaves of AM- and P_i-fertilized plants were not accompanied by transcriptional changes in CK biosynthesis (Table II). This can be explained by the fact that CKs also are synthesized in the root and translocated to the shoot (Sakakibara, 2006). The major transport form of CKs from root to shoot tissues is believed to be the conjugated CK form tZR (Kudo et al., 2010), which was found to be up-regulated in both AM- and P_i-fertilized plants as compared with controls. This hypothesis is in line with several studies reporting increased levels of CKs in both roots and shoots of AM plants (Fusconi, 2014). In addition, another conjugated form, tZ9G, was found to be up-regulated by both AM symbiosis and P_i fertilization, whereas AM specifically increased the free form DHZ (Fig. 3B).

We reported previously that AM- and P_i-fertilized *M. truncatula* plants had more and longer branches with larger and thicker leaflets and that only AM plants had a larger number of chloroplasts per cell section as compared with control plants (Adolfsson et al., 2015). CKs are known to promote cell division and branching as well as to support the development of chloroplasts (Cortleven and Schmülling, 2015). Hence, the observed increase of most CK metabolites may be the factor involved in remodeling the shoot architecture in AM and P_i plants, whereas the specific increase in DHZ may affect the chloroplast number.

JA Signaling May Play a Role in the AM-Induced Flavonoid and Terpenoid Biosynthesis

AM symbiosis, in contrast to P_i fertilization, stimulated the expression of genes involved in oxylipin biosynthesis in leaves (e.g. 9- and *13-LOX*, *AOS*, and *AOC*; Table II). 13-LOX isoforms, which share a strong similarity with the

chloroplast-localized AtLOX2, are dedicated to the biosynthesis of JA and its late precursor OPDA, while 9-LOXs are involved in the synthesis of JA-like molecules. Based on the observed AM-mediated transcriptional stimulation of the JA biosynthetic pathway, an increased content of JAs in AM leaves was expected. Instead, the content of the active conjugate JA-Ile was significantly lower in leaves of AM compared with control plants (Fig. 3B). It is reasonable to suggest that a transient increase of JA level in AM leaves could be sufficient to activate JA-responsive genes and downstream biosynthetic pathways. Indeed, the 24-h MeJA treatment of leaves of nonmycorrhized plants enhanced the expression of genes involved in JA biosynthesis (*AOS*) and signaling (*MYC2* and *JAZ*/MTR_5g013530) as well as the expression of genes involved in flavonoid (*LDOX* and *3′GT*) and terpenoid (*UGT73K1*) biosynthesis (Fig. 4), thus mimicking the effects of mycorrhization (Table II).

The lower level of JA-Ile in leaves of AM plants may be due to transport to distal tissues. Experimental evidence in Arabidopsis revealed the movement of JAs from wounded shoots toward roots, where they could affect defense gene expression (Gasperini et al., 2015). Such a long-distance transport of JAs has not yet been demonstrated for mycorrhized plants such as *M. truncatula*. Nevertheless, an increase in AM colonization was shown upon repeated wounding of *M. truncatula* leaves (a condition inducing JA biosynthesis) or following JA application to the shoot (Landgraf et al., 2012). In addition, many studies reported increases of JA levels in mycorrized roots of *M. truncatula*, which were accompanied by the up-regulation of JA biosynthesis and JA-induced responses, resulting in the establishment and maintenance of arbuscular mycorrhizas (for review, see Wasternack and Hause, 2013). Genes involved in JA biosynthesis also were found to be up-regulated in leaves of mycorrhized maize (*Zea mays*) plants (Gerlach et al., 2015). The previous works together with our observations (Table II; Fig. 4) support enhanced JA biosynthesis and signaling in both shoots and roots of mycorrhized plants and may involve the long-distance transport of JAs to ensure sufficient levels of root fungal colonization. In P_i-treated plants, the lower JA-Ile content coincides with the down-regulation of a few JA-responsive genes, including *MYC2* (Table II). This suggests that high P_i also affects JA signaling, but to lesser extent compared with mycorrhization.

AM symbiosis, in contrast to P_i fertilization, enhanced the level of ABA in leaves (Fig. 3B), in agreement with the up-regulation of genes involved in ABA biosynthesis and response (Table II). It has been reported that *MYC2* functions as a transcriptional activator of ABA signaling in Arabidopsis leaves under abiotic stress (Abe et al., 2003; Takagi et al., 2016). The crosstalk between ABA and JA has been shown to be regulated by MYC2 (Kazan and Manners, 2013). The mechanism behind this may involve the interaction between MYC2 and an ABA receptor in the presence of ABA, which could modify transcription driven by MYC2 in JA signaling pathways (Aleman et al., 2016). This could explain why, in our study, the 24-h ABA treatment of leaves did not alter the expression of *AOS*, *JAZ*/MTR_5g013530, or the JA-regulated flavonoid and terpenoid biosynthetic genes, despite the enhanced expression of *MYC2* (Fig. 4).

Based on our data, we propose a model of interactive pathways that modulate hormone levels, secondary metabolism, oxidative/iron stress, and ultimately growth in leaves of AM and P_i plants (Fig. 6). In this model, AM symbiosis promotes growth directly by enhancing CK levels and indirectly by stimulating MYC2-regulated JA and ABA signaling pathways in leaves. The JA signaling pathway for the biosynthesis of flavonoids, in turn, helps to chelate free Fe, thus improving fitness in oxidative stress. Possible ABA signaling pathways could be defense mechanisms for stomatal closure, induction of reactive oxygen species, and cell wall reinforcement during abiotic and biotic stress (Cameron et al., 2013). P_i fertilization also promotes growth via CKs and alleviates oxidative stress by a direct binding of free Fe to P_i. The proposed model contributes to enhanced functional insights into the AM fungus-plant interaction as well as the P_i-plant interaction at the shoot level and should be fully validated in future studies.

The results of MeJA and ABA application on leaves from nonmycorrhized plants (Fig. 4) demonstrate the role of these hormones in regulating flavonoid/anthocyanin production through *MYC2*-regulated pathways in *M. truncatula* and are in line with previous findings in the

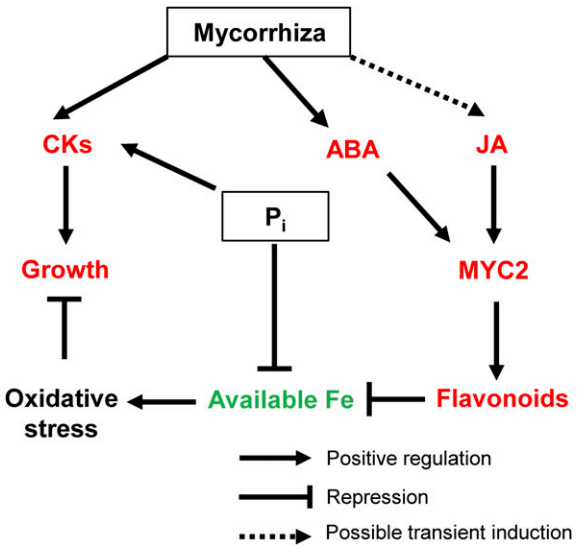

Figure 6. Proposed model of AM-regulated pathways in *M. truncatula* leaves. Mycorrhization enhances the level of ABA and possibly transiently the level of JA. Both JA and ABA activate the expression of the transcription factor *MYC2*. Only the JA-mediated activation in turn stimulates the expression of flavonoid-related genes. The resulting increase in flavonoids (including anthocyanins and proanthocyanidins) improves the scavenging of available iron. In P_i-fertilized plants, P_i binds directly to iron. Both mycorrhization and P_i fertilization increase the levels of CKs, which stimulate plant growth. Red and green colors indicate increase and decrease, respectively.

same and other plant species. Elicitor-induced transcription factors or JA application resulted in the reprogramming of secondary metabolism in *M. truncatula* (Naoumkina et al., 2008). In Arabidopsis, it has been shown that MeJA enhances anthocyanin content through the up-regulation of late biosynthetic genes including *DFR* and *LDOX* (Shan et al., 2009), a process in which the transcription factor AtMYC2 is the key regulator (Dombrecht et al., 2007). On the other hand, experiments in tomato fruits revealed the induction of early flavonoid biosynthesis genes in response to ABA application (Mou et al., 2015). Another work reported that ABA application on different organs of *Vitis vinifera* affects differently the expression of genes involved in different steps of flavonoid biosynthesis, which increased significantly only in berries (Rattanakon et al., 2016). In our study, although ABA treatment of leaves of nonmycorrhized plants up-regulated the expression of *MYC2*, it did not affect the expression of late flavonoid biosynthetic genes (Figs. 4 and 5). However, we cannot rule out the possibility that ABA produced in leaves of mycorrhized plants may interact with AM-induced JA pathways to regulate the expression of these genes. Therefore, it is reasonable to propose that MYC2 from *M. truncatula* might play a determinant role in the AM-mediated regulation of flavonoid biosynthesis. Taken together, AM-induced, JA- and ABA-regulated *MYC2* expression and CK production are beneficial for the growth and fitness of mycorrhized plants.

CONCLUSION

In this report, we show that AM symbiosis induces a secondary metabolism response in leaves of *M. truncatula*, mainly in phenylpropanoid and terpenoid biosynthesis. These pathways also were affected by P_i treatment, although some metabolites were altered in a converse manner compared with mycorrhization. The AM-mediated changes in leaves might have been triggered by MYC2 in a JA- and ABA-dependent manner. The use of a multilevel methodology, including transcriptomics, metabolomics, and phytohormone analysis, provided an overview of the changes in secondary and hormone metabolism occurring in leaves during root colonization by AM fungi. Detailed functional analyses using mutants affected in the respective biosynthetic pathways should further validate our hypotheses and might reveal additional factors involved in the signaling and regulation of growth in shoots of AM plants. Some of the identified regulated genes could serve as possible markers for such metabolic changes as those observed in our study.

In fine, the prospective question is the endogenous signal that stimulates ABA production. Such a chemical switch could be reactive oxygen species, whose inductive effect on ABA biosynthesis has been reported in leaves (Mittler et al., 2011). Further studies are needed to decipher in detail the sequential steps in the mycorrhiza-induced secondary and hormone metabolic responses.

MATERIALS AND METHODS

Biological Material and Growth Conditions

We used the growth conditions and protocols described previously by Adolfsson et al. (2015). Two-day-old *Medicago truncatula* 'Jemalong J5' seedlings that had germinated on agar plates were transplanted to soil consisting of Agsorb (24/48 LVMGA; Oil-Dri) and 30% (v/v) inoculum or mock inoculum. The inoculum consisted of a mixture of Agsorb and *Allium porum* (leek) roots either infected with the fungus *Rhizophagus irregularis* (syn. *Glomus intraradices*; Redecker et al., 2013) BEG 141 (AM plants) or not infected (control plants). The plants were grown in a CLF PlantMaster chamber (Plant Climatics) using a daily cycle of 16 h of light (400 μmol photons m^{-2} s^{-1}) at 25°C and 8 h of dark at 19°C and a relative humidity of 40%. Plants were watered once per week with a modified Long Ashton Nutrient Solution (*Medicago*-LANS; Hewitt, 1966), containing twice the amount of nitrate and no phosphate. Modified LANS medium supplemented with 5 mM NaH_2PO_4 was used for the P_i treatment, which was included to study the effects induced by high P_i supply, resulting in significantly increased (7-fold) leaf P content as compared with control and AM treatment (Table I). In some experiments, 1 mM P_i yielded nonsignificantly higher P levels than in control and AM plants (Supplemental Table S1).

Assessment of Root Mycorrhization

Young roots of AM plants were placed in 10% (w/v) KOH and incubated at 90°C for 45 min and thereafter incubated in black ink (90°C for 5 min; Vierheilig et al., 1998). The roots were then washed with tap water, dried, incubated in 8% (v/v) acetic acid at room temperature for 20 min, and finally rinsed with water. Afterward, the roots were cut in 30 pieces, mounted between slide and coverslide with glycerol at a distance of 0.5 to 1 mm, and analyzed with the Alphaphot-2 YS2 microscope (Nikon). The mycorrhizal colonization and the arbuscule abundance were estimated at 4 wpi using the formulas found on the Web page http://www2.dijon.inra.fr/mychintec (Trouvelot et al., 1986). This method was used to estimate the quality of plant-fungus symbiosis. In this study, plants were used at 4 weeks of age, when the mycorrhization was at maximum.

Phosphorus Determination

Dry shoot or leaf material was ground with a mortar. Soluble P_i content was measured after incubation in 1% (v/v) acetic acid at 42°C for 30 min. Total P (P_i and organic P) was measured after oxidizing organic P to P_i by incubating samples in an autoclave at 120°C for 1 h with an oxidation solution described by Valderrama (1981). P_i content was determined by colorimetric analysis using ammonium molybdate (Ames, 1966) and recalculated as mg of P.

Hormone Treatments

M. truncatula seeds were scarified and sterilized as described above. Sterilized seeds were sown on plates and transplanted into pots containing the same soil mixture and grown under the same conditions as described for nonmycorrhized plants. At the age of 4 wpi, plants were sprayed with either MeJA (Sigma-Aldrich) at concentrations of 100 μM and 1 mM or with ABA (Sigma-Aldrich) at concentrations of 10 and 100 μM in a solution also containing 0.1% (v/v) Triton X-100 and 1% (v/v) ethanol. Control plants for both hormone treatments were sprayed with a solution containing 0.1% (v/v) Triton X-100 and 1% (v/v) ethanol. Approximately 10 mL of solution was evenly sprayed over six plants. After spraying, pots were covered with lids. The middle lobe of the latest fully developed leaf of six replicate plants was harvested 24 h posttreatment and used for RNA extraction.

RNA Extraction

For microarray analyses, total RNA was extracted from leaflets of the latest fully developed leaf from *M. truncatula* control, AM-, and P_i-treated plants using the E.Z.N.A. Plant RNA Kit Standard protocol following the manufacturer's instructions (Omega Bio-Tek). The quality of RNA preparations was verified using the Agilent 2200 Bioanalyzer (Agilent Technologies). Both aforementioned RNA extraction and bioanalysis methods also were employed for experiments with ABA and MeJA treatments.

Microarray Analysis and Data Deposition

Total RNAs of control, P_i-, and AM-treated plants at 4 wpi were sent to the affiliated with the Karolinska Institute in Stockholm. Three biological replicates with one to two technical replicates per treatment were used. Total RNA was used to synthesize cyanine 3 labeled using Low Input Quick Amp Labeling according to the Agilent One-Color Gene Expression protocol. Labeled cRNA was purified, fragmented, and hybridized on Agilent *Medicago* Oligoarrays (8x60k) at 65°C under rotation in a hybridization oven. Array slides were washed with Gene Expression Wash buffers prior to drying. Fluorescent signals were measured with the G2505 C Micro Array Scanner (Agilent Technologies). Hybridization, washing steps, staining, and scanning were performed according to the manufacturer's instructions. Scanned images were analyzed with the Agilent Feature Extraction Software version 7.2. Resulting raw data were normalized (75th quantile, median to baseline of all samples).

Microarray data analysis was performed using Analyst software (Genedata). Raw data were normalized using the Lowess algorithm to identify regulated genes. A threshold of 2 for transcript ratio in treatment versus control, $P < 0.01$ (Student's t test), and $Q < 0.05$ (false discovery rate multiple-test correction [Benjamin and Hochberg, 1995] as an indicator of false-positive significant genes) were set as criteria for the selection of regulated genes in AM- and P_i-fertilized plants as compared with control (nonmycorrhized) plants. The genes following a common pattern of expression (up-regulated/down-regulated) were grouped together. Further gene annotation was performed through the National Center for Biotechnology Information database (https://blast.ncbi.nlm.nih.gov/Blast.cgi). After the statistical analysis, when more than one significant probe sets matched the same gene identifier, redundant probe sets were randomly removed for simplicity. We did not observe opposite trends (both up- and down-regulation) within significant redundant probe sets. Classification of candidate genes was implemented according to Journet et al. (2002) and by manual inspection. Common features were determined with the Venny program (http://bioinfogp.cnb.csic.es/tools/venny/index.html). The full data set is publicly available from the Gene Expression Omnibus repository at the National Center for Biotechnology Information (Barrett et al., 2007) with accession number GSE80610.

Quantitative RT-PCR

To confirm the microarray results, the expression levels of 13 selected genes were investigated using quantitative RT-PCR. In addition, *MtTef-1a*, whose expression was found to be constant in all treatments (control, P_i, and AM), was used as a reference gene for normalization of expression data for the selected genes. Sequences of primers designed using Primer 3 software (flypush.imgen.bcm.tmc.edu/primer/primer3_www.cgi) are given in Supplemental Table S12.

Total RNA was used as a template to synthesize cDNA using the iScript cDNA kit according to the manufacturer's instructions (Bio-Rad Laboratories). Next, cDNAs served as probes for quantitative PCR gene expression analysis using the Perfecta SYBR Green SuperMix kit (Roxtm). Three to four biological replicates and two technical replicates for each gene of interest were investigated. The cycle threshold values of quantitative PCR were used to normalize the expression levels of target genes with the expression level of the reference gene from *M. truncatula* (Kakar et al., 2008). The gene expression levels in leaves of AM- and P_i-treated plants were compared with the control condition.

Determination of Available Fe

Fe was extracted according to Everett et al. (2014) as follows. Dried leaf samples (20–60 mg) were soaked in 1 M HCl overnight at room temperature under gentle shaking; extracted Fe is referred to as available Fe. Then, samples were allowed to stand for 10 min, and the liquid phase was centrifuged at 400g and filtered. For the determination of available Fe(II), 150 μL of the samples was mixed with 150 μL of the extraction solution. Fe(III) was determined after reduction to Fe(II) with 50% (v/v) hydroxylamine hydrochloride. Both reduced and nonreduced samples were added to 2 mM Ferrozine in 50 mM potassium acetate buffer (pH 5.5). For each sample, the background was determined in the potassium acetate buffer and subtracted from the Ferrozine-based values. Equivalent volumes of 1 M HCl and hydroxylamine hydrochloride in 1 M HCl were used as blanks for nonreduced and reduced samples, respectively.

Total Flavonoid and Anthocyanin Content Analyses

Frozen leaves (30–60 mg) were transferred to Eppendorf tubes and ground using a pestle. After adding 1 mL of acidic methanol (3% [v/v] formic acid), samples were homogenized, and the tubes were incubated at 4°C overnight with continuous gentle shaking in the dark. Then, samples were centrifuged, the supernatant was transferred into a 15-mL Falcon tube, and the pellet was resuspended with 500 μL of acidic methanol twice and incubated for 10 min in the dark to fully extract anthocyanins. Combined supernatants were mixed with 1 mL of deionized water and 2 mL of chloroform. After centrifugation at 4,000g for 5 min, the upper organic phase enriched in anthocyanins was collected. The experiments were carried out in four replicates. Total flavonoid content was determined by the chloride colorimetric assay (Jia et al., 1999) and expressed according to the standard curve of quercetin at an absorbance of 510 nm. Anthocyanin content was measured by reading the A_{530} with a spectrophotometer using the pH differential method (buffers of 0.025 M KCl [pH 1] and 0.4 M sodium acetate [pH 4.5]). A standard curve of purified cyanidin 3-*O*-glucoside chloride (Sigma-Aldrich), one of the major anthocyanins in *M. truncatula*, was used as a reference.

Metabolomic Analysis

Metabolites were extracted from 20 mg of leaves for each treatment in 1 mL of methanol, chloroform, and water (20:60:20, v/v) including internal standards (Gullberg et al., 2004). A total of 200 μL of each sample was dried, dissolved in 20 μL of methanol, and then diluted with 20 μL of water.

The chromatographic separation was performed using an Agilent 1290 Infinity UHPLC system, where 2 μL of shoot extract was injected onto an Acquity UPLC HSS T3 column (2.1 × 50 mm, 1.8 μm C_{18}) at 40°C. The gradient elution was A (water, 0.1% formic acid (v/v)) and B (75:25 acetonitrile:2-propanol, 0.1% formic acid v/v) as follows: 0.1% to 10% B (v/v) over 2 min, B was increased to 99% (v/v) over 5 min, and then held at 99% (v/v) for 2 min, returning to 0.1% (v/v) for 0.3 to 0.9 min; the flow rate was 0.5 mL min^{-1}. The compounds were detected with an Agilent 6540 Q-TOF mass spectrometer equipped with an electrospray ion source operating in positive ion mode. A reference interface was connected for accurate mass measurements; the gas temperature was set to 300°C, the drying gas flow to 8 L min^{-1}, and the nebulizer pressure to 40 psig. The sheath gas temperature was set to 350°C and the sheath gas flow to 11 L min^{-1}. The capillary voltage was set to 4,000 V and the nozzle voltage was 0 V. The fragmentor voltage was 100 V, the skimmer was 45 V, and the octopole RF (OCT 1 RF Vpp) was 750 V. The collision energy was set to 0 V. The m/z range was 70 to 1,700, and data were collected in centroid mode with an acquisition rate of four scans per second. The tandem mass spectrometry (MS/MS) spectra were obtained in the same conditions, with the collision energy from 10 to 40 V. The generated mass files were processed using Profinder B.06.00 (Agilent Technologies) using mass feature extraction and find-by-ion algorithms for peak detection. Mass Profiler Professional 12.5 (Agilent Technologies) was used to compile the extracted data into a data table for statistical analysis. The generated data were normalized against the internal standard and weight of each sample (Supplemental Table S8).

The metabolites were identified by manual interpretation of the high mass accuracy of fragments produced by MS/MS experiments and/or metabolite and mass spectra library database search. The OPLS-DA (Trygg and Wold, 2002) were performed using SIMCA 13.0 software comparing control with AM and P_i treatments. Valid statistical models consisted of $Q^2 \geq 0.05$ (Supplemental Fig. S2A). The VIP plot (Variable Importance for the Projection) in a confidence level of 95% was used to summarize how many variables explain the models. Valid models discriminate control from AM or 5 mM P_i, and the SUS (Shared and Unique Structures) plot (Wiklund et al., 2008) between them was used to select metabolites with similar or unique trends under 5 mM P_i and AM conditions. Based on the Q^2, the comparison between control and 1 mM P_i did not result in a valid model. However, by selecting 17% of the metabolites (164 out of 988) on the basis of the VIP plot, a significant model was produced. The low percentage of variable metabolites in the 1 mM P_i model (contrasting with 28% for 5 mM Pi or 32% for AM) suggests minor changes in secondary metabolites under such low-P_i concentration, which make it indistinguishable from the control. Instead, the main changes under such low-P_i concentration might be in the primary rather than in the secondary metabolites. In this case, techniques other than liquid chromatography-mass spectrometry (LC-MS) could be more appropriate.

The significant metabolites from the discriminant analyses as well as their respective P (Student's t test) and Q (false discovery rate multiple-test correction calculated according to Benjamin and Hochberg [1995]) values are listed in Supplemental Table S9 for evaluation of the goodness of the results, and those exhibiting significant changes in treatments versus control ($Q < 0.05$) are presented in Table III.

Plant Hormone Analysis by Ultra-HPLC Tandem Electrospray Mass Spectrometry

The extraction and purification of plant hormones were carried out in six biological replicates. Samples were homogenized under liquid N_2, and the amount corresponding to 20 mg fresh weight of material per sample was used for the analyses of CKs, JAs, ABA, and SA. The amount of sample corresponding to 10 mg fresh weight was used for the analysis of auxins.

CKs were extracted in modified Bieleski buffer (methanol:water:formic acid, 15:4:1, v/v/v) and then purified using two solid-phase extraction columns, a C18 octadecylsilica-based column (500 mg of sorbent; Applied Separations) and, after that, an Oasis MCX column (30 mg of mixed-mode sorbent with reversed-phase/cation-exchange properties; Waters; Dobrev and Kamínek, 2002). Auxins were extracted in 1 mL of cold 50 mM sodium phosphate buffer (pH 7) containing 1% diethyldithiocarbamic acid sodium salt (w/v). After extraction, samples were divided in half, using one-half for derivatization of labile indole-3-pyruvic acid by 0.25 M cysteamine (pH 8). Both fractions of the extract were purified by solid-phase extraction using Oasis HLB columns (30 mg mL^{-1}; Waters). JAs, ABA, and SA were extracted using an aqueous solution of methanol (10% methanol:water, v/v) and purified using Oasis HLB columns (30 mg mL^{-1}; Waters).

Levels of the CKs, auxins, and JAs together with SA and ABA were determined by the isotope dilution method using ultra-HPLC tandem electrospray mass spectrometry with stable isotope-labeled internal standards used as a reference (Novák et al., 2012; Svačinová et al., 2012; Floková et al., 2014).

The determined absolute concentrations of analytes (pmol g^{-1} fresh weight) were used to create a data set. The variables with more than 50% of missing values (values below the limit of detection) were removed from the data set. The variables containing up to 50% of missing values were replaced by two-thirds of the minimum of a group. The data were treated and statistically evaluated by SIMCA software (version 14; Umetrics). Pareto scaling and logarithmic transformation were applied to all data variables. Multivariate statistical analysis such as PCA and OPLS-DA were performed. Unsupervised PCA was used to give a general overview and observe trends of the data structure. To discriminate variables responsible for group separation, always two groups (control versus AM or control versus P_i treated) were compared by supervised OPLS-DA. An OPLS-DA S-plot was used for visualization. It combines covariance (p1; the farther the distance from zero, the higher the contribution to the difference between two groups) and correlation (pcorr1; the farther the distance from zero, the higher the reliability).

Statistics

All statistical analyses, except when stated, were conducted using one-way ANOVA with Fisher's LSD as a posterior test in GraphPad Prism 5 (GraphPad Software). Student's *t* test and multiple-test correction were conducted using Mass Profiler Professional 13.0 (Agilent Technologies and Strand Life Sciences). Supplemental Table S1 provides an experimental overview with the types of analyses performed, conditions, and number of replicates.

Supplemental Data

The following supplemental materials are available.

Supplemental Figure S1. Representative photographs of plants, which were nonmycorrhized, infected with AM, or treated with 5 mM P_i at 4 wpi.

Supplemental Figure S2. OPLS-DA performed on a metabolomic data set generated from the LC-MS analysis.

Supplemental Figure S3. MS/MS spectra for the Na adduct of the molecular ion with *m/z* 433.2404, tentatively identified as dihydroxy blumenol glucoside.

Supplemental Figure S4. OPLS-DA S-plots of the hormone data set generated from the LC-MS analysis.

Supplemental Table S1. Experimental overview.

Supplemental Table S2. List of AM up-regulated genes.

Supplemental Table S3. List of AM down-regulated genes.

Supplemental Table S4. List of P_i up-regulated genes.

Supplemental Table S5. List of P_i down-regulated genes.

Supplemental Table S6. Common significantly regulated genes by AM and P_i treatment

Supplemental Table S7. Comparison of gene expression data from microarray analyses and quantitative RT-PCR.

Supplemental Table S8. Relative abundance of metabolites detected by liquid chromatography-time of flight-mass spectrometry.

Supplemental Table S9. Annotation of metabolites.

Supplemental Table S10. Phytohormone levels detected by the ultra-HPLC tandem electrospray mass spectrometry method.

Supplemental Table S11. Gene expression data from quantitative RT-PCR following hormone application.

Supplemental Table S12. List of primer sequences used for quantitative RT-PCR analysis.

ACKNOWLEDGMENTS

We thank the Bioinformatics and Expression Analysis core facility at Novum, affiliated with the Karolinska Institute in Stockholm, for the microarray analyses; the Swedish Metabolomic Centre (www.swedishmetabolomicscentre.se) for access to the LC-MS instrumentation; and Jarmila Greplová, Eva Hirnerová, and Ivan Petřík for technical support and sample preparation during the plant hormone analyses.

Received September 29, 2016; accepted July 7, 2017; published July 11, 2017.

LITERATURE CITED

Abdallah C, Valot B, Guillier C, Mounier A, Balliau T, Zivy M, van Tuinen D, Renaut J, Wipf D, Dumas-Gaudot E, et al (2014) The membrane proteome of *Medicago truncatula* roots displays qualitative and quantitative changes in response to arbuscular mycorrhizal symbiosis. J Proteomics **108:** 354–368

Abe H, Urao T, Ito T, Seki M, Shinozaki K, Yamaguchi-Shinozaki K (2003) *Arabidopsis* AtMYC2 (bHLH) and AtMYB2 (MYB) function as transcriptional activators in abscisic acid signaling. Plant Cell **15:** 63–78

Achnine L, Huhman DV, Farag MA, Sumner LW, Blount JW, Dixon RA (2005) Genomics-based selection and functional characterization of triterpene glycosyltransferases from the model legume *Medicago truncatula*. Plant J **41:** 875–887

Adolfsson L, Solymosi K, Andersson MX, Keresztes Á, Uddling J, Schoefs B, Spetea C (2015) Mycorrhiza symbiosis increases the surface for sunlight capture in *Medicago truncatula* for better photosynthetic production. PLoS ONE **10:** e0115314

Aleman F, Yazaki J, Lee M, Takahashi Y, Kim AY, Li Z, Kinoshita T, Ecker JR, Schroeder JI (2016) An ABA-increased interaction of the PYL6 ABA receptor with MYC2 transcription factor: a putative link of ABA and JA signaling. Sci Rep **6:** 28941

Aliferis KA, Chamoun R, Jabaji S (2015) Metabolic responses of willow (Salix purpurea L.) leaves to mycorrhization as revealed by mass spectrometry and ^{1}H NMR spectroscopy metabolite profiling. Front Plant Sci **6:** 344

Ames BN (1966) Assay of inorganic phosphate, total phosphate and phosphatases. Methods Enzymol **8:** 115–118

An JP, Li HH, Song LQ, Su L, Liu X, You CX, Wang XF, Hao YJ (2016) The molecular cloning and functional characterization of MdMYC2, a bHLH transcription factor in apple. Plant Physiol Biochem **108:** 24–31

Arnaud N, Murgia I, Boucherez J, Briat JF, Cellier F, Gaymard F (2006) An iron-induced nitric oxide burst precedes ubiquitin-dependent protein degradation for Arabidopsis AtFer1 ferritin gene expression. J Biol Chem **281:** 23579–23588

Arosio P, Ingrassia R, Cavadini P (2009) Ferritins: a family of molecules for iron storage, antioxidation and more. Biochim Biophys Acta **1790:** 589–599

Baier MC, Keck M, Gödde V, Niehaus K, Küster H, Hohnjec N (2010) Knockdown of the symbiotic sucrose synthase MtSucS1 affects arbuscule maturation and maintenance in mycorrhizal roots of *Medicago truncatula*. Plant Physiol **152:** 1000–1014

Barrett T, Troup DB, Wilhite SE, Ledoux P, Rudnev D, Evangelista C, Kim IF, Soboleva A, Tomashevsky M, Edgar R (2007) NCBI GEO: mining tens of millions of expression profiles—database and tools update. Nucleic Acids Res **35:** D760–D765

Benjamin Y, Hochberg Y (1995) Controlling the false discovery rate: a practical and powerful approach to multiple testing. J R Stat Soc B **57:** 289–300

Cameron DD, Neal AL, van Wees SCM, Ton J (2013) Mycorrhiza-induced resistance: more than the sum of its parts? Trends Plant Sci **18:** 539–545

Cheng X, Ruyter-Spira C, Bouwmeester H (2013) The interaction between strigolactones and other plant hormones in the regulation of plant development. Front Plant Sci **4:** 199

Chugh A, Ray A, Gupta JB (2003) Squalene epoxidase as hypocholesterolemic drug target revisited. Prog Lipid Res **42:** 37–50

Cook DR (1999) *Medicago truncatula*: a model in the making! Curr Opin Plant Biol **2:** 301–304

Cortleven A, Schmülling T (2015) Regulation of chloroplast development and function by cytokinin. J Exp Bot **66:** 4999–5013

Daher Z, Recorbet G, Solymosi K, Wienkoop S, Mounier A, Morandi D, Lherminier J, Wipf D, Dumas-Gaudot E, Schoefs B (2017) Changes in plastid proteome and structure in arbuscular mycorrhizal roots display a nutrient starvation signature. Physiol Plant **159:** 13–29

Deguchi Y, Banba M, Shimoda Y, Chechetka SA, Suzuri R, Okusako Y, Ooki Y, Toyokura K, Suzuki A, Uchiumi T, et al (2007) Transcriptome profiling of Lotus japonicus roots during arbuscular mycorrhiza development and comparison with that of nodulation. DNA Res **14:** 117–133

Ding L, Xu H, Yi H, Yang L, Kong Z, Zhang L, Xue S, Jia H, Ma Z (2011) Resistance to hemi-biotrophic *F. graminearum* infection is associated with coordinated and ordered expression of diverse defense signaling pathways. PLoS ONE **6:** e19008

Dobrev PI, Kamínek M (2002) Fast and efficient separation of cytokinins from auxin and abscisic acid and their purification using mixed-mode solid-phase extraction. J Chromatogr A **950:** 21–29

Doidy J, van Tuinen D, Lamotte O, Corneillat M, Alcaraz G, Wipf D (2012) The Medicago truncatula sucrose transporter family: characterization and implication of key members in carbon partitioning towards arbuscular mycorrhizal fungi. Mol Plant **5:** 1346–1358

Dombrecht B, Xue GP, Sprague SJ, Kirkegaard JA, Ross JJ, Reid JB, Fitt GP, Sewelam N, Schenk PM, Manners JM, et al (2007) MYC2 differentially modulates diverse jasmonate-dependent functions in *Arabidopsis*. Plant Cell **19:** 2225–2245

Everett J, Céspedes E, Shelford LR, Exley C, Collingwood JF, Dobson J, van der Laan G, Jenkins CA, Arenholz E, Telling ND (2014) Ferrous iron formation following the co-aggregation of ferric iron and the Alzheimer's disease peptide β-amyloid (1-42). J R Soc Interface **11:** 20140165

Fernie AR, Stitt M (2012) On the discordance of metabolomics with proteomics and transcriptomics: coping with increasing complexity in logic, chemistry, and network interactions scientific correspondence. Plant Physiol **158:** 1139–1145

Finkelstein R (2013) Abscisic acid synthesis and response. The Arabidopsis Book **11:** e0166

Fiorilli V, Catoni M, Miozzi L, Novero M, Accotto GP, Lanfranco L (2009) Global and cell-type gene expression profiles in tomato plants colonized by an arbuscular mycorrhizal fungus. New Phytol **184:** 975–987

Floková K, Tarkowská D, Miersch O, Strnad M, Wasternack C, Novák O (2014) UHPLC-MS/MS based target profiling of stress-induced phytohormones. Phytochemistry **105:** 147–157

Floss DS, Hause B, Lange PR, Küster H, Strack D, Walter MH (2008) Knockdown of the MEP pathway isogene 1-deoxy-D-xylulose 5-phosphate synthase 2 inhibits formation of arbuscular mycorrhiza-induced apocarotenoids, and abolishes normal expression of mycorrhiza-specific plant marker genes. Plant J **56:** 86–100

Fukushima EO, Seki H, Sawai S, Suzuki M, Ohyama K, Saito K, Muranaka T (2013) Combinatorial biosynthesis of legume natural and rare triterpenoids in engineered yeast. Plant Cell Physiol **54:** 740–749

Fusconi A (2014) Regulation of root morphogenesis in arbuscular mycorrhizae: what role do fungal exudates, phosphate, sugars and hormones play in lateral root formation? Ann Bot (Lond) **113:** 19–33

Gasperini D, Chauvin A, Acosta IF, Kurenda A, Stolz S, Chételat A, Wolfender JL, Farmer EE (2015) Axial and radial oxylipin transport. Plant Physiol **169:** 2244–2254

Gehrig H, Schüssler A, Kluge M (1996) *Geosiphon pyriforme*, a fungus forming endocytobiosis with Nostoc (cyanobacteria), is an ancestral member of the Glomales: evidence by SSU rRNA analysis. J Mol Evol **43:** 71–81

Gerlach N, Schmitz J, Polatajko A, Schlüter U, Fahnenstich H, Witt S, Fernie AR, Uroic K, Scholz U, Sonnewald U, et al (2015) An integrated functional approach to dissect systemic responses in maize to arbuscular mycorrhizal symbiosis. Plant Cell Environ **38:** 1591–1612

Gholami A, De Geyter N, Pollier J, Goormachtig S, Goossens A (2014) Natural product biosynthesis in Medicago species. Nat Prod Rep **31:** 356–380

Gomez SK, Cox MM, Bede JC, Inoue K, Alborn HT, Tumlinson JH, Korth KL (2005) Lepidopteran herbivory and oral factors induce transcripts encoding novel terpene synthases in *Medicago truncatula*. Arch Insect Biochem Physiol **58:** 114–127

Grunwald U, Guo W, Fischer K, Isayenkov S, Ludwig-Müller J, Hause B, Yan X, Küster H, Franken P (2009) Overlapping expression patterns and differential transcript levels of phosphate transporter genes in arbuscular mycorrhizal, Pi-fertilised and phytohormone-treated *Medicago truncatula* roots. Planta **229:** 1023–1034

Guether M, Neuhäuser B, Balestrini R, Dynowski M, Ludewig U, Bonfante P (2009) A mycorrhizal-specific ammonium transporter from *Lotus japonicus* acquires nitrogen released by arbuscular mycorrhizal fungi. Plant Physiol **150:** 73–83

Güimil S, Chang HS, Zhu T, Sesma A, Osbourn A, Roux C, Ioannidis V, Oakeley EJ, Docquier M, Descombes P, et al (2005) Comparative transcriptomics of rice reveals an ancient pattern of response to microbial colonization. Proc Natl Acad Sci USA **102:** 8066–8070

Gullberg J, Jonsson P, Nordström A, Sjöström M, Moritz T (2004) Design of experiments: an efficient strategy to identify factors influencing extraction and derivatization of *Arabidopsis thaliana* samples in metabolomic studies with gas chromatography/mass spectrometry. Anal Biochem **331:** 283–295

Harrison MJ, Dixon RA (1994) Spatial patterns of expression of flavonoid/isoflavonoid pathway genes during interactions between roots of *Medicago truncatula* and the mycorrhizal fungus *Glomus versiforme*. Plant J **6:** 9–20

Hewitt EJ (1966) Sand and Water Culture Methods Used in the Study of Plant Nutrition, Ed 2. Commonwealth Agricultural Bureaux, Farnham Royal, UK

Hohnjec N, Vieweg MF, Pühler A, Becker A, Küster H (2005) Overlaps in the transcriptional profiles of *Medicago truncatula* roots inoculated with two different Glomus fungi provide insights into the genetic program activated during arbuscular mycorrhiza. Plant Physiol **137:** 1283–1301

Hou X, Rivers J, León P, McQuinn RP, Pogson BJ (2016) Synthesis and function of apocarotenoid signals in plants. Trends Plant Sci **21:** 792–803

Isayenkov S, Mrosk C, Stenzel I, Strack D, Hause B (2005) Suppression of allene oxide cyclase in hairy roots of *Medicago truncatula* reduces jasmonate levels and the degree of mycorrhization with *Glomus intraradices*. Plant Physiol **139:** 1401–1410

Jaakola L (2013) New insights into the regulation of anthocyanin biosynthesis in fruits. Trends Plant Sci **18:** 477–483

Jia Z, Tang MC, Wu JM (1999) The determination of flavonoid contents in mulberry and their scavenging effects on superoxide radicals. Food Chem **64:** 555–559

Jiang JR, Yuan S, Ding JF, Zhu SC, Xu HD, Chen T, Cong XD, Xu WP, Ye H, Dai YJ (2008) Conversion of puerarin into its 7-O-glycoside derivatives by Microbacterium oxydans (CGMCC 1788) to improve its water solubility and pharmacokinetic properties. Appl Microbiol Biotechnol **81:** 647–657

Jin CW, Ye YQ, Zheng SJ (2014) An underground tale: contribution of microbial activity to plant iron acquisition via ecological processes. Ann Bot (Lond) **113:** 7–18

Journet EP, van Tuinen D, Gouzy J, Crespeau H, Carreau V, Farmer MJ, Niebel A, Schiex T, Jaillon O, Chatagnier O, et al (2002) Exploring root symbiotic programs in the model legume *Medicago truncatula* using EST analysis. Nucleic Acids Res **30:** 5579–5592

Kakar K, Wandrey M, Czechowski T, Gaertner T, Scheible WR, Stitt M, Torres-Jerez I, Xiao Y, Redman JC, Wu HC, et al (2008) A community resource for high-throughput quantitative RT-PCR analysis of transcription factor gene expression in *Medicago truncatula*. Plant Methods **4:** 18

Kazan K, Manners JM (2013) MYC2: the master in action. Mol Plant **6:** 686–703

Kim SA, Punshon T, Lanzirotti A, Li L, Alonso JM, Ecker JR, Kaplan J, Guerinot ML (2006) Localization of iron in Arabidopsis seed requires the vacuolar membrane transporter VIT1. Science **314:** 1295–1298

Kobayashi T, Nishizawa NK (2012) Iron uptake, translocation, and regulation in higher plants. Annu Rev Plant Biol **63:** 131–152

Kudo T, Kiba T, Sakakibara H (2010) Metabolism and long-distance translocation of cytokinins. J Integr Plant Biol **52:** 53–60

Landgraf R, Schaarschmidt S, Hause B (2012) Repeated leaf wounding alters the colonization of *Medicago truncatula* roots by beneficial and pathogenic microorganisms. Plant Cell Environ **35:** 1344–1357

Larose G, Chenevert R, Moutoglis P, Gagne S, Piche Y, Vierheilig H (2002) Flavonoid levels in roots of *Medicago sativa* are modulated by the developmental stage of the symbiosis and the root colonizing arbuscular mycorrhizal fungus. J Plant Physiol **159:** 1329–1339

León Morcillo RJ, Ocampo JA, García Garrido JM (2012) Plant 9-LOX oxylipin metabolism in response to arbuscular mycorrhiza. Plant Signal Behav **7:** 1584–1588

Li J, Dai X, Liu T, Zhao PX (2012) LegumeIP: an integrative database for comparative genomics and transcriptomics of model legumes. Nucleic Acids Res **40:** D1221–D1229

Liu J, Blaylock LA, Endre G, Cho J, Town CD, VandenBosch KA, Harrison MJ (2003) Transcript profiling coupled with spatial expression analyses reveals genes involved in distinct developmental stages of an arbuscular mycorrhizal symbiosis. Plant Cell **15:** 2106–2123

Liu J, Maldonado-Mendoza I, Lopez-Meyer M, Cheung F, Town CD, Harrison MJ (2007) Arbuscular mycorrhizal symbiosis is accompanied by local and systemic alterations in gene expression and an increase in disease resistance in the shoots. Plant J **50:** 529–544

López-Ráez JA, Verhage A, Fernández I, García JM, Azcón-Aguilar C, Flors V, Pozo MJ (2010) Hormonal and transcriptional profiles highlight common and differential host responses to arbuscular mycorrhizal fungi and the regulation of the oxylipin pathway. J Exp Bot **61:** 2589–2601

Luo ZB, Janz D, Jiang X, Göbel C, Wildhagen H, Tan Y, Rennenberg H, Feussner I, Polle A (2009) Upgrading root physiology for stress tolerance by ectomycorrhizas: insights from metabolite and transcriptional profiling into reprogramming for stress anticipation. Plant Physiol **151:** 1902–1917

Mira L, Fernandez MT, Santos M, Rocha R, Florêncio MH, Jennings KR (2002) Interactions of flavonoids with iron and copper ions: a mechanism for their antioxidant activity. Free Radic Res **36:** 1199–1208

Miransari M, Abrishamchi A, Khoshbakht K, Niknam V (2014) Plant hormones as signals in arbuscular mycorrhizal symbiosis. Crit Rev Biotechnol **34:** 123–133

Mittler R, Vanderauwera S, Suzuki N, Miller G, Tognetti VB, Vandepoele K, Gollery M, Shulaev V, Van Breusegem F (2011) ROS signaling: the new wave? Trends Plant Sci **16:** 300–309

Morita M, Shibuya M, Kushiro T, Masuda K, Ebizuka Y (2000) Molecular cloning and functional expression of triterpene synthases from pea (*Pisum sativum*) new alpha-amyrin-producing enzyme is a multifunctional triterpene synthase. Eur J Biochem **267:** 3453–3460

Mou W, Li D, Luo Z, Mao L, Ying T (2015) Transcriptomic analysis reveals possible influences of ABA on secondary metabolism of pigments, flavonoids and antioxidants in tomato fruit during ripening. PLoS ONE **10:** e0129598

Mouradov A, Spangenberg G (2014) Flavonoids: a metabolic network mediating plants adaptation to their real estate. Front Plant Sci **5:** 620

Nadeem SM, Ahmad M, Zahir ZA, Javaid A, Ashraf M (2014) The role of mycorrhizae and plant growth promoting rhizobacteria (PGPR) in improving crop productivity under stressful environments. Biotechnol Adv **32:** 429–448

Naoumkina MA, He X, Dixon RA (2008) Elicitor-induced transcription factors for metabolic reprogramming of secondary metabolism in *Medicago truncatula*. BMC Plant Biol **8:** 132

Nesi N, Jond C, Debeaujon I, Caboche M, Lepiniec L (2001) The *Arabidopsis* TT2 gene encodes an R2R3 MYB domain protein that acts as a key determinant for proanthocyanidin accumulation in developing seed. Plant Cell **13:** 2099–2114

Nishio JN, Abadía J, Terry N (1985) Chlorophyll-proteins and electron transport during iron nutrition-mediated chloroplast development. Plant Physiol **78:** 296–299

Novák O, Hényková E, Sairanen I, Kowalczyk M, Pospíšil T, Ljung K (2012) Tissue-specific profiling of the *Arabidopsis thaliana* auxin metabolome. Plant J **72:** 523–536

Orino K, Lehman L, Tsuji Y, Ayaki H, Torti SV, Torti FM (2001) Ferritin and the response to oxidative stress. Biochem J **357:** 241–247

Plaza M, Pozzo T, Liu J, Gulshan Ara KZ, Turner C, Nordberg Karlsson E (2014) Substituent effects on in vitro antioxidizing properties, stability, and solubility in flavonoids. J Agric Food Chem **62:** 3321–3333

Rasmussen L, Toftlund H (1986) Phosphate compounds as iron chelators in animal cell cultures. In Vitro Cell Dev Biol **22:** 177–179

Rattanakon S, Ghan R, Gambetta GA, Deluc LG, Schlauch KA, Cramer GR (2016) Abscisic acid transcriptomic signaling varies with grapevine organ. BMC Plant Biol **16:** 72

Ravet K, Touraine B, Boucherez J, Briat JF, Gaymard F, Cellier F (2009) Ferritins control interaction between iron homeostasis and oxidative stress in Arabidopsis. Plant J **57:** 400–412

Redecker D, Schüssler A, Stockinger H, Stürmer SL, Morton JB, Walker C (2013) An evidence-based consensus for the classification of arbuscular mycorrhizal fungi (Glomeromycota). Mycorrhiza **23:** 515–531

Rivas-San Vicente M, Plasencia J (2011) Salicylic acid beyond defence: its role in plant growth and development. J Exp Bot **62:** 3321–3338

Rooney DC, Killham K, Bending GD, Baggs E, Weih M, Hodge A (2009) Mycorrhizas and biomass crops: opportunities for future sustainable development. Trends Plant Sci **14:** 542–549

Sakakibara H (2006) Cytokinins: activity, biosynthesis, and translocation. Annu Rev Plant Biol **57:** 431–449

Scervino JM, Ponce MA, Erra-Bassells R, Vierheilig H, Ocampo JA, Godeas A (2005) Flavonoids exhibit fungal species and genus specific effects on the presymbiotic growth of Gigaspora and Glomus. Mycol Res **109:** 789–794

Schachtman DP, Reid RJ, Ayling SM (1998) Phosphorus uptake by plants: from soil to cell. Plant Physiol **116:** 447–453

Schliemann W, Ammer C, Strack D (2008) Metabolite profiling of mycorrhizal roots of *Medicago truncatula*. Phytochemistry **69:** 112–146

Schnepf A, Roose T, Schweiger P (2008) Impact of growth and uptake patterns of arbuscular mycorrhizal fungi on plant phosphorus uptake: a modelling study. Plant Soil **312:** 85–99

Schussler A, Schwarzott D, Walker C (2001) A new fungal phylum, the Glomeromycota: phylogeny and evolution. Mycol Res **105:** 1413–1421

Schweiger R, Baier MC, Müller C (2014a) Arbuscular mycorrhiza-induced shifts in foliar metabolism and photosynthesis mirror the developmental stage of the symbiosis and are only partly driven by improved phosphate uptake. Mol Plant Microbe Interact **27:** 1403–1412

Schweiger R, Baier MC, Persicke M, Müller C (2014b) High specificity in plant leaf metabolic responses to arbuscular mycorrhiza. Nat Commun **5:** 3886

Shan X, Zhang Y, Peng W, Wang Z, Xie D (2009) Molecular mechanism for jasmonate-induction of anthocyanin accumulation in Arabidopsis. J Exp Bot **60:** 3849–3860

Siciliano V, Genre A, Balestrini R, Cappellazzo G, deWit PJGM, Bonfante P (2007) Transcriptome analysis of arbuscular mycorrhizal roots during development of the prepenetration apparatus. Plant Physiol **144:** 1455–1466

Smith SE, Jakobsen I, Grønlund M, Smith FA (2011) Roles of arbuscular mycorrhizas in plant phosphorus nutrition: interactions between pathways of phosphorus uptake in arbuscular mycorrhizal roots have important implications for understanding and manipulating plant phosphorus acquisition. Plant Physiol **156:** 1050–1057

Smith SE, Smith FA, Jakobsen I (2004) Functional diversity in arbuscular mycorrhizal (AM) symbioses: the contribution of the mycorrhizal P uptake pathway is not correlated with mycorrhizal responses in growth or total P uptake. New Phytol **162:** 511–524

Song YY, Ye M, Li C, He X, Zhu-Salzman K, Wang RL, Su YJ, Luo SM, Zeng RS (2014) Hijacking common mycorrhizal networks for herbivore-induced defence signal transfer between tomato plants. Sci Rep **4:** 3915

Spíchal L (2012) Cytokinins: recent news and views of evolutionally old molecules. Funct Plant Biol **39:** 267–284

Stookey LL (1970) Ferrozine: a new spectrophotometric reagent for iron. Anal Chem **42:** 779

Stumpe M, Carsjens JG, Stenzel I, Göbel C, Lang I, Pawlowski K, Hause B, Feussner I (2005) Lipid metabolism in arbuscular mycorrhizal roots of *Medicago truncatula*. Phytochemistry **66:** 781–791

Suzuki H, Achnine L, Xu R, Matsuda SPT, Dixon RA (2002) A genomics approach to the early stages of triterpene saponin biosynthesis in *Medicago truncatula*. Plant J **32:** 1033–1048

Svačinová J, Novák O, Plačková L, Lenobel R, Holík J, Strnad M, Doležal K (2012) A new approach for cytokinin isolation from Arabidopsis tissues using miniaturized purification: pipette tip solid-phase extraction. Plant Methods **8:** 17

Takagi H, Ishiga Y, Watanabe S, Konishi T, Egusa M, Akiyoshi N, Matsuura T, Mori IC, Hirayama T, Kaminaka H, et al (2016) Allantoin, a stress-related purine metabolite, can activate jasmonate signaling in a MYC2-regulated and abscisic acid-dependent manner. J Exp Bot **67:** 2519–2532

Takeda K (2006) Blue metal complex pigments involved in blue flower color. Proc Jpn Acad Ser B Phys Biol Sci **82:** 142–154

Thimmappa R, Geisler K, Louveau T, O'Maille P, Osbourn A (2014) Triterpene biosynthesis in plants. Annu Rev Plant Biol **65:** 225–257

Tholl D (2015) Biosynthesis and biological functions of terpenoids in plants. Adv Biochem Eng Biotechnol **148:** 63–106

Trouvelot A, Fardeau JC, Plenchette C, Gianinazzi S, Gianinazzapearson V (1986) Nutritional balance and symbiotic expression in mycorrhizal wheat. Physiol Veg **24:** 300

Trygg J, Wold S (2002) Orthogonal projections to latent structures (O-PLS). J Chemometr **16:** 119–128

Valderrama JC (1981) The simultaneous analysis of total nitrogen and total phosphorus in natural waters. Mar Chem **10:** 109–122

Vanstraelen M, Benková E (2012) Hormonal interactions in the regulation of plant development. Annu Rev Cell Dev Biol **28:** 463–487

Vierheilig H, Coughlan AP, Wyss U, Piche Y (1998) Ink and vinegar, a simple staining technique for arbuscular-mycorrhizal fungi. Appl Environ Microbiol **64:** 5004–5007

Walter MH, Floss DS, Strack D (2010) Apocarotenoids: hormones, mycorrhizal metabolites and aroma volatiles. Planta **232:** 1–17

Wasternack C, Hause B (2013) Jasmonates: biosynthesis, perception, signal transduction and action in plant stress response, growth and development. An update to the 2007 review in Annals of Botany. Ann Bot (Lond) **111:** 1021–1058

Wiklund S, Johansson E, Sjöström L, Mellerowicz EJ, Edlund U, Shockcor JP, Gottfries J, Moritz T, Trygg J (2008) Visualization of GC/TOF-MS-based metabolomics data for identification of biochemically interesting compounds using OPLS class models. Anal Chem **80:** 115–122

Wulf A, Manthey K, Doll J, Perlick AM, Linke B, Bekel T, Meyer F, Franken P, Küster H, Krajinski F (2003) Transcriptional changes in response to arbuscular mycorrhiza development in the model plant *Medicago truncatula*. Mol Plant Microbe Interact **16:** 306–314

Xiong L, Zhu JK (2003) Regulation of abscisic acid biosynthesis. Plant Physiol **133:** 29–36

Yan Y, Borrego E, Kolomiets MV (2013) Jasmonate biosynthesis, perception and function in plant development and stress responses. *In* PRV Baez, ed, Lipid Metabolism. InTech Rijeka, pp. 393–442